# UDRC Summer School 2021: Source Separation and Beamforming

Stephan Weiss

Centre for Signal & Image Processing
Department of Electonic & Electrical Engineering
University of Strathclyde, Glasgow, Scotland, UK

UDRC Summer School, 1 July 2021

With many thanks to:
J.G. McWhirter, I.K. Proudler, J. Pestana, J. Corr, Z. Wang, F.K. Coutts, C. Delaosa, and F. Khattak

This work was supported by the Engineering and Physical Sciences Research Council (EPSRC) Grant number EP/S000631/1 and the MOD University Defence Research Collaboration in Signal Processing.

# Polynomial Matrix Co-Enthusiasts

# Presentation Overview

1. Overview

## Part I: Polynomial Matrices and Decompositions

2. Polynomial matrices and basic operations
   2.1 occurence: MIMO systems, filter banks, space-time covariance
   2.2 basic properties and operations
3. Polynomial eigenvalue decomposition (PEVD)
4. Iterative PEVD algorithms
   4.1 sequential best rotation (SBR2)
   4.2 sequential matrix diagonalisation (SMD)
5. PEVD Matlab toolbox

## Part II: Beamforming & Source Separation Applications

6. Broadband MIMO decoupling
7. Broadband angle of arrival estimation
8. Broadband beamforming
9. Source-sensor transfer function extraction from 2nd order statistics
10. Summary and materials

# What is a Polynomial Matrix?

- A polynomial matrix is a polynomial with matrix-valued coefficients, e.g.:

$$\boldsymbol{A}(z) = \begin{bmatrix} 1 & -1 \\ -1 & 2 \end{bmatrix} + \begin{bmatrix} 1 & 1 \\ 1 & -1 \end{bmatrix} z^{-1} + \begin{bmatrix} -1 & 2 \\ 1 & -1 \end{bmatrix} z^{-2} \quad (1)$$

- a polynomial matrix can equivalently be understood a matrix with polynomial entries, i.e.

$$\boldsymbol{A}(z) = \begin{bmatrix} 1 + z^{-1} - z^{-2} & -1 + z^{-1} + 2z^{-2} \\ -1 + z^{-1} + z^{-2} & 2 - z^{-1} - z^{-2} \end{bmatrix} \quad (2)$$

- polynomial matrices could also contain rational polynomials, but the notation would not be as easily interchangeable as (1) and (2).

# Where Do Polynomial Matrices Arise?

- A multiple-input multiple-output (MIMO) system could be made up of a number of finite impulse response (FIR) channels:

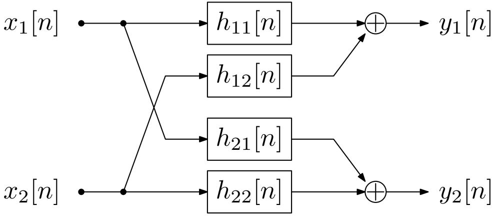


- writing this as a matrix of impulse responses:

$$\mathbf{H}[n] = \begin{bmatrix} h_{11}[n] & h_{12}[n] \\ h_{21}[n] & h_{22}[n] \end{bmatrix} \tag{3}$$

# Transfer Function of a MIMO System

- Example for MIMO matrix $\mathbf{H}[n]$ of impulse responses:

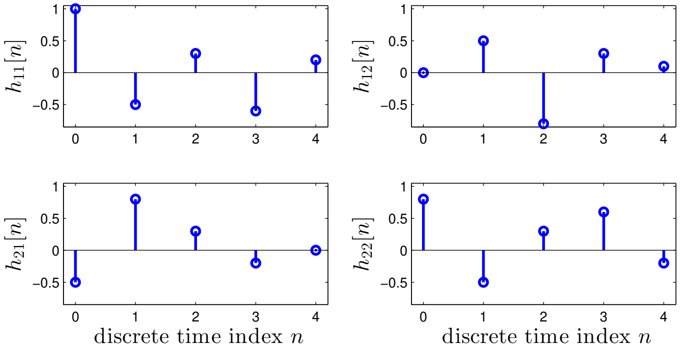


- the transfer function of this MIMO system is a polynomial matrix:

$$\boldsymbol{H}(z) = \sum_{n=-\infty}^{\infty} \mathbf{H}[n] z^{-1} \qquad \text{or} \qquad \boldsymbol{H}(z) \bullet\!\!-\!\!\circ \mathbf{H}[n] \qquad (4)$$

# Analysis Filter Bank

- Critically decimated $K$-channel analysis filter bank:

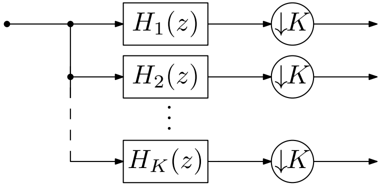


- equivalent polyphase representation:

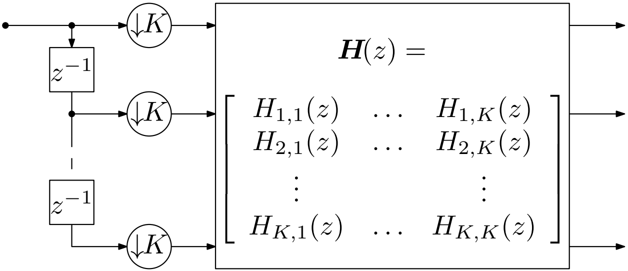

# Polyphase Analysis Matrix

- With the $K$-fold polyphase decomposition of the analysis filters

$$H_k(z) = \sum_{n=1}^{K} H_{k,n}(z^K) z^{-n+1} \qquad (5)$$

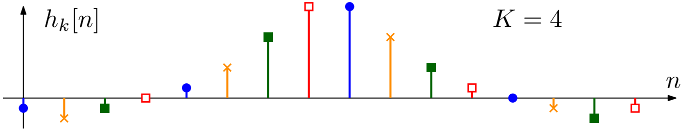


- the polyphase analysis matrix is a polynomial matrix:

$$\boldsymbol{H}(z) = \begin{bmatrix} H_{1,1}(z) & H_{1,2}(z) & \dots & H_{1,K}(z) \\ H_{2,1}(z) & H_{2,2}(z) & \dots & H_{2,K}(z) \\ \vdots & \vdots & \ddots & \vdots \\ H_{K,1}(z) & H_{K,2}(z) & \dots & H_{K,K}(z) \end{bmatrix} \qquad (6)$$

# Synthesis Filter Bank

- Critically decimated $K$-channel synthesis filter bank:

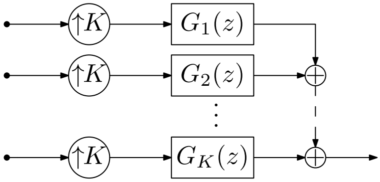


- equivalent polyphase representation:

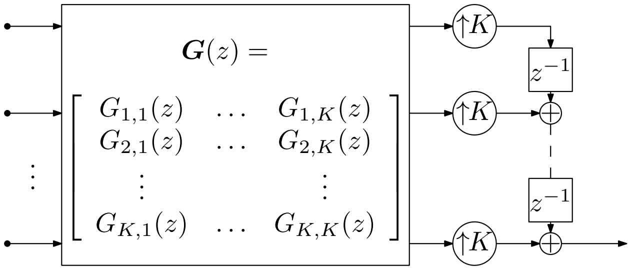

# Polyphase Synthesis Matrix

- Analoguous to analysis filter bank, the synthesis filters $G_k(z)$ can be split into $K$ polyphase components, creating a polyphse synthesis matrix

$$\boldsymbol{G}(z) = \begin{bmatrix} G_{1,1}(z) & G_{1,2}(z) & \dots & G_{1,K}(z) \\ G_{2,1}(z) & G_{2,2}(z) & \dots & G_{2,K}(z) \\ \vdots & \vdots & \ddots & \vdots \\ G_{K,1}(z) & G_{K,2}(z) & \dots & G_{K,K}(z) \end{bmatrix} \quad (7)$$

- operating analysis and synthesis back-to-back, perfect reconstruction is achieved if

$$\boldsymbol{G}(z)\boldsymbol{H}(z) = \mathbf{I} \; ; \quad (8)$$

- i.e. for perfect reconstruction, the polyphase analysis matrix must be invertible: $\boldsymbol{G}(z) = \boldsymbol{H}^{-1}(z)$.

# Space-Time Covariance Matrix

- Measurements obtained from $M$ sensors are collected in a vector $\mathbf{x}[n] \in \mathbb{C}^M$:

$$\mathbf{x}^{\mathrm{T}}[n] = [x_1[n] \;\; x_2[n] \;\; \ldots \;\; x_M[n]] \;; \tag{9}$$

- with the expectation operator $\mathcal{E}\{\cdot\}$, the spatial correlation is captured by $\mathbf{R} = \mathcal{E}\{\mathbf{x}[n]\mathbf{x}^{\mathrm{H}}[n]\}$;
- for spatial and temporal correlation, we require a space-time covariance matrix

$$\mathbf{R}[\tau] = \mathcal{E}\{\mathbf{x}[n]\mathbf{x}^{\mathrm{H}}[n-\tau]\} \tag{10}$$

- this space-time covariance matrix contains auto- and cross-correlation terms, e.g. for $M = 2$

$$\mathbf{R}[\tau] = \left[ \begin{array}{cc} \mathcal{E}\{x_1[n]x_1^*[n-\tau]\} & \mathcal{E}\{x_1[n]x_2^*[n-\tau]\} \\ \mathcal{E}\{x_2[n]x_1^*[n-\tau]\} & \mathcal{E}\{x_2[n]x_2^*[n-\tau]\} \end{array} \right] \tag{11}$$

# Cross-Spectral Density Matrix

- example for a space-time covariance matrix $\mathbf{R}[\tau] \in \mathbb{R}^{2\times 2}$:

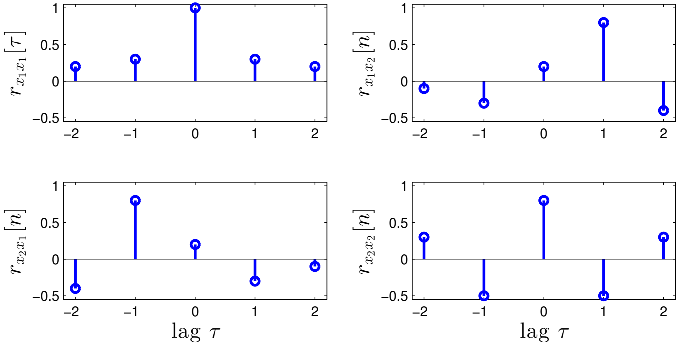


- the cross-spectral density (CSD) matrix

$$\boldsymbol{R}(z) \circ\!\!-\!\!\bullet \mathbf{R}[\tau] \qquad (12)$$

is a polynomial matrix.

# Parahermitian Operator

- A parahermitian operation is indicated by $\{\cdot\}^{\mathrm{P}}$, and compared to the Hermitian (= complex conjugate transpose) of a matrix additionally performs a time-reversal;
- example:

$\boldsymbol{A}(z) =$

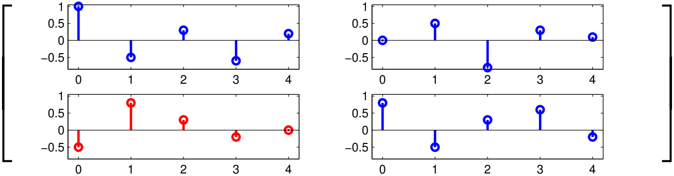


- parahermitian $\boldsymbol{A}^{\mathrm{P}}(z) = \boldsymbol{A}^{\mathrm{H}}(1/z^*)$:

$\boldsymbol{A}^{\mathrm{P}}(z) =$

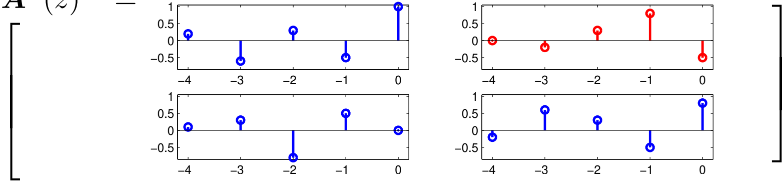

# Parahermitian Property

- A polynomial matrix $\boldsymbol{R}(z)$ is parahermitian if $\boldsymbol{R}^{\mathrm{P}}(z) = \boldsymbol{R}^{\mathrm{H}}(1/z^*) = \boldsymbol{R}(z)$;
- this is an extension of the symmetric (if $\mathbf{R} \in \mathbb{R}$) or or Hermitian (if $\mathbf{R} \in \mathbb{C}$) property to the polynomial case: transposition, complex conjugation and time reversal (in any order) do not alter a parahermitian $\boldsymbol{R}(z)$;
- any CSD matrix is parahermitian;
- example:

$\boldsymbol{R}(z) =$

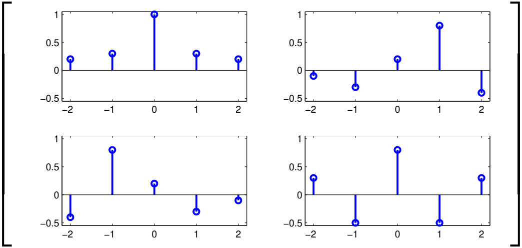


$= \boldsymbol{R}^{\mathrm{P}}(z)$

# Paraunitary Matrices

- Recall that $\mathbf{A} \in \mathbb{C}$ (or $\mathbf{A} \in \mathbb{R}$) is a unitary (or orthonormal) matrix if $\mathbf{A}\mathbf{A}^{\mathrm{H}} = \mathbf{A}^{\mathrm{H}}\mathbf{A} = \mathbf{I}$;
- in the polynomial case, $\mathbf{A}(z)$ is paraunitary if

$$\boldsymbol{A}(z)\boldsymbol{A}^{\mathrm{P}}(z) = \boldsymbol{A}^{\mathrm{P}}(z)\boldsymbol{A}(z) = \mathbf{I} \qquad (13)$$

- therefore, if $\boldsymbol{A}(z)$ is paraunitary, then the polynomial matrix inverse is simple:

$$\boldsymbol{A}^{-1}(z) = \boldsymbol{A}^{\mathrm{P}}(z) \qquad (14)$$

- example: polyphase analysis or synthesis matrices of perfectly reconstructing (or lossless) filter banks are usually paraunitary.

# Attempt at Gaussian Elimination

- System of polynomial equations:

$$\begin{bmatrix} A_{11}(z) & A_{12}(z) \\ A_{21}(z) & A_{22}(z) \end{bmatrix} \cdot \begin{bmatrix} X_1(z) \\ X_2(z) \end{bmatrix} = \begin{bmatrix} B_1(z) \\ B_2(z) \end{bmatrix} \qquad (15)$$

- modification of 2nd row:

$$\begin{bmatrix} A_{11}(z) & A_{12}(z) \\ A_{11}(z) & \frac{A_{11}(z)}{A_{21}(z)} A_{22}(z) \end{bmatrix} \cdot \begin{bmatrix} X_1(z) \\ X_2(z) \end{bmatrix} = \begin{bmatrix} B_1(z) \\ \frac{A_{11}(z)}{A_{21}(z)} B_2(z) \end{bmatrix} \qquad (16)$$

- upper triangular form by subtracting 1st row from 2nd:

$$\begin{bmatrix} A_{11}(z) & A_{12}(z) \\ 0 & \frac{A_{11}(z)A_{22}(z) - A_{12}(z)A_{21}(z)}{A_{21}(z)} \end{bmatrix} \cdot \begin{bmatrix} X_1(z) \\ X_2(z) \end{bmatrix} = \begin{bmatrix} B_1(z) \\ \bar{B}_2(z) \end{bmatrix} \qquad (17)$$

- penalty: we end up with rational polynomials.

# Further Reading

- General polynomial matrices and operations [45, 52];
- polyphase analysis and synthesis matrices in the context of multirate systems and filter banks [92, 93, 42];
- space-time covariance matrices [93, 58, 76];
- estimation of space-time covariance matrices [38, 39, 40].

# Polynomial Eigenvalue Decomposition

(McWhirter Decomposition [58])

- Polynomial EVD of the CSD matrix

$$\boldsymbol{R}(z) \approx \hat{\boldsymbol{U}}(z)\, \hat{\boldsymbol{\Gamma}}(z)\, \hat{\boldsymbol{U}}^{\mathrm{P}}(z) \qquad (18)$$

- with paraunitary $\hat{\boldsymbol{U}}(z)$, s.t. $\hat{\boldsymbol{U}}(z)\hat{\boldsymbol{U}}^{\mathrm{P}}(z) = \mathbf{I}$;
- diagonalised and spectrally majorised $\hat{\boldsymbol{\Gamma}}(z)$:

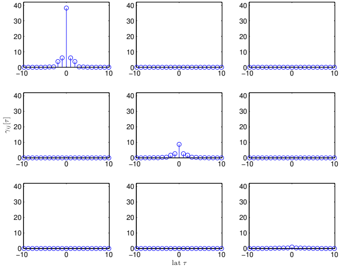


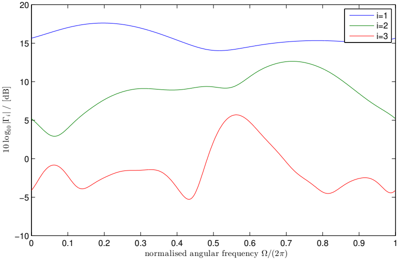


- algorithms exist, with proven convergence; but we previously did not know to what values these converge.

# Source Model for CSD Matrix

- General source model for a CSD matrix with $L$ unit variance, uncorrelated and mutually independent inputs $u_\ell[n]$, $\ell = 1 \ldots L$, and $M$ measurements $x_m[n]$, $m = 1 \ldots M$:

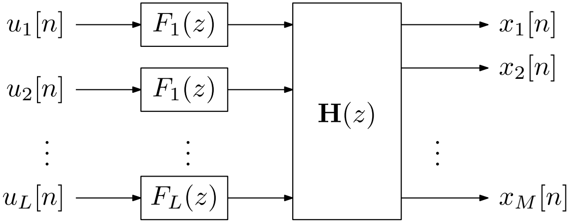


- source PSDs via innovation filter: $S_\ell(z) = F_\ell(z)F_\ell^{\mathrm{P}}(z)$;
- for the CSD matrix:

$$\boldsymbol{R}(z) = \boldsymbol{H}(z)\boldsymbol{F}(z)\boldsymbol{F}^{\mathrm{P}}(z)\boldsymbol{H}^{\mathrm{P}}(z) \ . \tag{19}$$

# Definitions around the CSD Matrix

- The innovation filters $F_\ell(z)$ and $\boldsymbol{H}(z)$ can be polynomials or rational functions in $z$, but are assumed to be causal and stable;
- they can be represented as a power series (or matrix of power series), $n \in \mathbb{N}$,

$$X(z) = \sum_n x_n z^{-n}$$

- we have a Laurent series, if $n \in \mathbb{Z}$;
- power and Laurent series do not need to converge (=absolutely summable, $\sum_n |x_n| < \infty$);
- they are analytic if they converge;
- if the sums are finite, we speak of polynomials ($n \in \mathbb{N}$) and Laurent polynomials ($n \in \mathbb{Z}$);
- $\mathbf{R}(z)$ is a Laurent series, and analytic in an annulus $\mathcal{D}$;
- analyticity: $\boldsymbol{R}(z)$ is infinitely differentiable.

# Eigenvalue Decomposition (EVD)

- A Hermitian matrix $\mathbf{R} = \mathbf{R}^{\mathrm{H}}$ be positive semidefinite (given for any covariance matrix, or anything arising from $\mathbf{R} = \mathbf{A}\mathbf{A}^{\mathrm{H}}$, with $\mathbf{A}$ arbitary);
- eigenvalues and eigenvectors:

$$\mathbf{R}\mathbf{q}_m = \lambda_m \mathbf{q}_m$$

- eigenvalues $\lambda \in \mathbb{R}$, $\lambda \geq 0$;
- eigenvectors are chosen to be orthonormal, but have an arbitary phase shift: $\mathbf{q}'_m = e^{j\varphi}\mathbf{q}_m$ is also an eigenvector;
- in case of an algebraic multiplicity $C$: $\lambda_m = \lambda_{m+1} = \cdots = \lambda_{m+C-1}$, only a $C$-dimensional subspace is defined, within which the eigenvectors can form an arbitrary orthonormal basis, with any unitary $\mathbf{V}$:

$$[\mathbf{q}'_m, \ \ldots \ \mathbf{q}'_{m+C-1}] = [\mathbf{q}_m, \ \ldots \ \mathbf{q}_{m+C-1}]\,\mathbf{V} \ , \tag{20}$$

# Problem Statement

- We want to investigate the existence and uniquess of the EVD of a positive semidefinite parahermitian matrix $\boldsymbol{R}(z)$ [104, 103]:

$$\boldsymbol{R}(z) = \boldsymbol{U}(z)\,\boldsymbol{\Gamma}(z)\,\boldsymbol{U}^{\mathrm{P}}(z)\ , \tag{21}$$

- $\boldsymbol{U}(z)$ must be paraunitary;
- $\boldsymbol{\Gamma}(z)$ must be diagonal and parahermitian.
- we call this a parahermitian matrix EVD;
- why do we care about the $z$-domain representation? If we can write $\boldsymbol{U}(z)$ and $\boldsymbol{\Gamma}(z)$ as convergent power/Laurent series, we can immediately derive time domain realisations $\mathbf{U}[n]$ and $\boldsymbol{\Gamma}[n]$.

# EVD on the Unit Circle

- Analyticity: $\boldsymbol{R}(z)$ is uniquely definited by its representation on the unit circle, $\boldsymbol{R}(e^{j\Omega} = \boldsymbol{R}(z)|_{z=e^{j\Omega}}$;
- $\boldsymbol{R}(e^{j\Omega})$ is self-adjoint: $\boldsymbol{R}(e^{j\Omega}) = \boldsymbol{R}^{\mathrm{H}}(e^{j\Omega})$, i.e. Hermitian for every $\Omega$;
- EVD on the unit circle [82, 103]:

$$\boldsymbol{R}(e^{j\Omega}) = \boldsymbol{Q}(e^{j\Omega})\boldsymbol{\Lambda}(e^{j\Omega})\boldsymbol{Q}^{\mathrm{H}}(e^{j\Omega}) \ . \tag{22}$$

- for every $\Omega$, $\boldsymbol{Q}(e^{j\Omega})$ and $\boldsymbol{\Lambda}(e^{j\Omega})$ fulfill the properties of the EVD;
- can we find $\mathbf{U}(z)$ and $\boldsymbol{\Gamma}(z)$ such that on the unit circle

$$\mathbf{U}(e^{j\Omega}) = \boldsymbol{Q}(e^{j\Omega}) \tag{23}$$

$$\boldsymbol{\Gamma}(e^{j\Omega}) = \boldsymbol{\Lambda}(e^{j\Omega}) \tag{24}$$

- all now depends on the continuity/smoothness of $\boldsymbol{Q}(e^{j\Omega})$ and $\boldsymbol{\Lambda}(e^{j\Omega})$;

University of Strathclyde Engineering

# Matrix Perturbation Theory

- If we know that $\boldsymbol{R}(e^{j\Omega})$ varies smoothly, what can be say about $\boldsymbol{Q}(e^{j\Omega})$ and $\boldsymbol{\Lambda}(e^{j\Omega})$?
- eigenvalues (Hoffman-Wielandt, 1953):

$$\sum_i |\lambda_i(e^{j\Omega}) - \lambda_i(e^{j(\Omega+\Delta\Omega)})| \leq \|\boldsymbol{R}(e^{j\Omega}) - \boldsymbol{R}(e^{j(\Omega+\Delta\Omega)})\|_{\mathrm{F}} \ , \quad (25)$$

- eigenvector subspace [46]:

$$\boldsymbol{Q}^{\mathrm{H}}(e^{j\Omega}) \left( \boldsymbol{R}(e^{j(\Omega+\Delta\Omega)}) - \boldsymbol{R}(e^{j\Omega}) \right) \boldsymbol{Q}(e^{j\Omega}) = \left[ \begin{array}{cc} \underbrace{\begin{array}{c} \mathbf{E}_{11}(e^{j\Omega}, \Delta\Omega) \\ \mathbf{E}_{21}(e^{j\Omega}, \Delta\Omega) \end{array}}_{C} & \underbrace{\begin{array}{c} \mathbf{E}_{21}^{\mathrm{H}}(e^{j\Omega}, \Delta\Omega) \\ \mathbf{E}_{22}(e^{j\Omega}, \Delta\Omega) \end{array}}_{M-C} \end{array} \right] . \quad (26)$$

$$\mathrm{dist}\{\mathcal{Q}_1(e^{j\Omega}), \mathcal{Q}_1(e^{j(\Omega+\Delta\Omega)})\} \leq \frac{4}{\delta} \|\mathbf{E}_{21}(e^{j\Omega}, \Delta\Omega)\|_{\mathrm{F}} \ . \quad (27)$$

# Weierstrass (1885)

- As long as $\boldsymbol{Q}(e^{j\Omega})$ is continuous, it can be arbitrarily closely approximated by a converging series of polynomials;
- the functions may change as the approximation order changes;
- hence there is not just one function in the limit;
- we would like something more precise, and ideally obtain an approximant by truncating the limit function.

# Analytic EVD

- Franz Rellich (1937) for a self-adjoint, analytic $\boldsymbol{R}(e^{j\Omega})$:

$$\boldsymbol{R}(e^{j\Omega}) = \boldsymbol{Q}(e^{j\Omega})\boldsymbol{\Lambda}(e^{j\Omega})\boldsymbol{Q}^{\mathrm{H}}(e^{j\Omega}) \ ;$$

- $\boldsymbol{Q}(e^{j\Omega})$ and $\boldsymbol{\Lambda}(e^{j\Omega})$ *can* be chosen analytic;
- similarly for an arbitrary (i.e. not necessarily Hermitian or even square) analytic matrix, Boyd & de Moor (1989) and Bunse-Gerstner (1991) established an analytic SVD.

# Eigenvalue Considerations

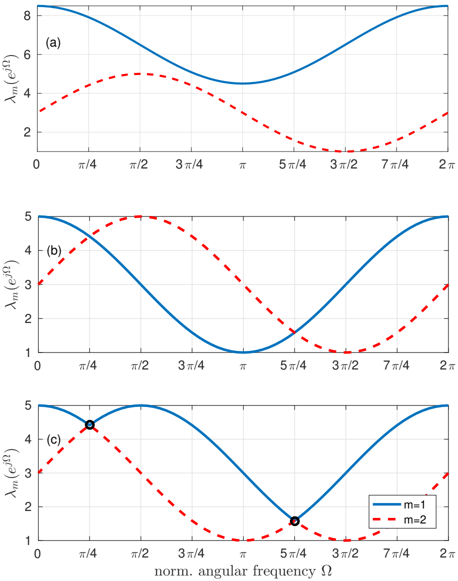


We distinguish three cases:

- non-overlapping eigenvalues $\lambda_m(e^{j\Omega})$, where all eigenvalues have algebraic multiplicity one for all frequencies $\Omega$;
- overlapping, maximally smooth eigenvalues;
- overlapping, spectrally majorised PSDs.

# Distinct Eigenvalues — Eigenvalues

- Since $\lambda_m(e^{j\Omega}) \in \mathbb{R}$ we can write

$$\hat{\lambda}_m^{(N)}(e^{j\Omega}) = \sum_{\ell=0}^{N} c_\ell e^{j\ell\Omega} + c_\ell^* e^{-j\ell\Omega}, \quad c_\ell \in \mathbb{C}\,; \tag{28}$$

- with $\hat{\mathbf{\Lambda}}^{(N)}(e^{j\Omega}) = \text{diag}\left\{\hat{\lambda}_1^{(N)}(e^{j\Omega}),\ \ldots\ ,\hat{\lambda}_M^{(N)}(e^{j\Omega})\right\}$, uniform convergence implies that for every $\epsilon_\Lambda > 0$ there exists $N_0 > 0$ such that (Stone-Weierstrass)

$$\sup_{\Omega\in[0,2\pi)} \left\|\hat{\mathbf{\Lambda}}^{(N)}(e^{j\Omega}) - \mathbf{\Lambda}(e^{j\Omega})\right\| < \epsilon_\Lambda, \tag{29}$$

- this requires Hölder continuity for $\mathbf{\Lambda}(e^{j\Omega})$:

$$|X(e^{j\Omega_1}) - X(e^{j\Omega_2})| \leq C|e^{j\Omega_1} - e^{j\Omega_2}|^\alpha \tag{30}$$

University of Strathclyde Engineering

# Analytic Eigenvalues

- We had

$$\hat{\lambda}_m^{(N)}(e^{j\Omega}) = \sum_{\ell=0}^{N} c_\ell e^{j\ell\Omega} + c_\ell^* e^{-j\ell\Omega}, \quad c_\ell \in \mathbb{C} \;;$$

- for absolutely summability $\sum_\ell |c_\ell| < \infty$, we require a slightly stricter form of Hölder with $\alpha > \frac{1}{2}$;
- then there exist unique eigenvalues of a parahermitian matrix:

$$\gamma_m(z) = \sum_{\ell=-\infty}^{\infty} c_\ell z^{-\ell}$$

- these are generally infinite sums or transcendental functions in $z$ (Weierstrass);
- an arbitrarily close approximation by Laurent polynomials is possible via truncation:

$$\hat{\gamma}_m(z) = \sum_{\ell=-N}^{N} c_\ell z^{-\ell}$$

# Example of a $2 \times 2$ Matrix

- Given an arbitrary parahermitian $\boldsymbol{R}(z) \in \mathbb{C}^{2\times 2}$;
- eigenvalues $\gamma_{1,2}(z)$ can be directly computed in the $z$-domain as the roots of

$$\det\{\gamma(z)\mathbf{I} - \boldsymbol{R}(z)\} = \gamma^2(z) - T(z)\gamma(z) + D(z) = 0$$

- determinant $D(z) = \det\{\boldsymbol{R}(z)\}$ and trace $T(z) = \mathrm{trace}\{\boldsymbol{R}(z)\}$;
- this leads to

$$\gamma_{1,2}(z) = \frac{1}{2}T(z) \pm \frac{1}{2}\sqrt{T(z)T^{\mathrm{P}}(z) - 4D(z)}\;; \qquad (31)$$

- awkward: $T(z)T^{\mathrm{P}}(z) - 4D(z) = S(z)S^{\mathrm{P}}(z)$ is parahermitian, but so must be the result of the square root.

University of Strathclyde Engineering

# Example cont'd

- Colin Maclaurin to the rescue: for every root of $S(z)$,

$$\sqrt{1-\beta z^{-1}} = \sum_{n=0}^{\infty} \xi_n \beta^n z^{-n} \qquad (32)$$

$$\frac{1}{\sqrt{1-\alpha z^{-1}}} = \left( \sum_{n=0}^{\infty} \xi_n \alpha^n z^{-n} \right)^{-1} \qquad (33)$$

$$= \sum_{n=0}^{\infty} \chi_n \alpha^n z^{-n} \qquad (34)$$

- with coefficients

$$\xi_n = (-1)^n \binom{\frac{1}{2}}{n} = \frac{(-1)^n}{n!} \prod_{i=0}^{n-1} \left( \frac{1}{2} - i \right) \ , \qquad (35)$$

$$\chi_n = (-1)^n \binom{-\frac{1}{2}}{n} = \frac{(-1)^{n-1}}{n!} \prod_{i=0}^{n-1} \left( \frac{1}{2} + i \right) \ . \qquad (36)$$

# Example cont'd

- Coefficients $\xi_n$ and $\chi_n$ for $n = 0 \ldots 50$:

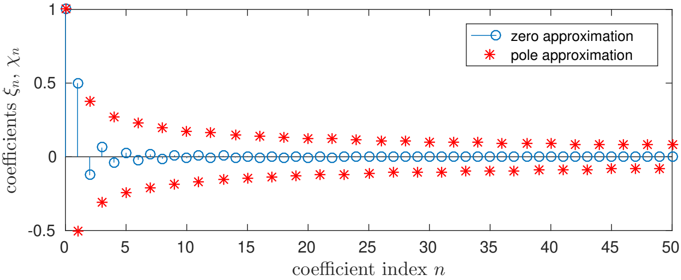


- these coefficients additionally dampen a geometric series;
- only if $S(z)$ has double zeros (and double poles) is a polynomial (rational) solution possible;
- in general, the result are transcendental eigenvalues.

# Numerical Example

Example from Icart & Comon (2012):

$$\boldsymbol{R}(z) = \begin{bmatrix} 1 & 1 \\ 1 & -2z + 6 - 2z^{-1} \end{bmatrix}$$

- solution on unit circle;
- coefficients of analytic eigenvalues;
- decay of coefficients.

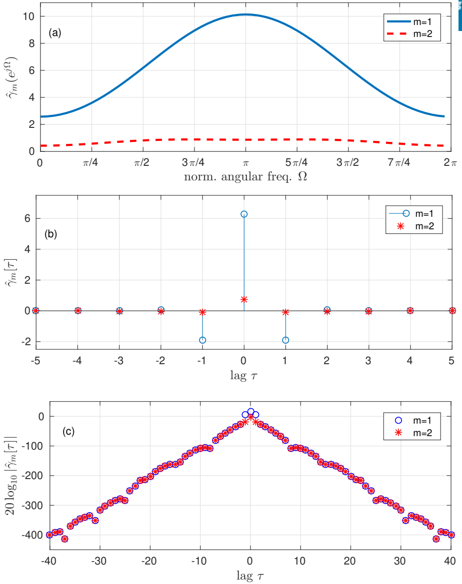

# Eigenvectors

- Recall: eigenvectors $\boldsymbol{q}_m(e^{j\Omega})$ have an arbitrary phase response;
- if this phase response is Hölder continuous, analytic eigenvectors exists; some phase ambiguity remains;
- if the phase response is discontiunous at $\Omega_0$,

$$\lim_{N\to\infty} \hat{\boldsymbol{q}}_m^{(N)}(e^{j\Omega_0}) = \frac{1}{2}\lim_{\Omega\to 0}\Big(\boldsymbol{q}_m(e^{j(\Omega_0-\Omega)}) + \\ + \ \boldsymbol{q}_m(e^{j(\Omega_0+\Omega)})\Big) \ ; \qquad (37)$$

  but this Fourier series does converge neither uniformly nor absolutely; analytic eigenvalues do not exist;
- there is a grey area (continuous but not Hölder) where we cannot make any statement;
- analytic approximations are possible in both cases.

# Overlapping Eigenvalues

- We now inspect the case of overlapping eigenvalues:

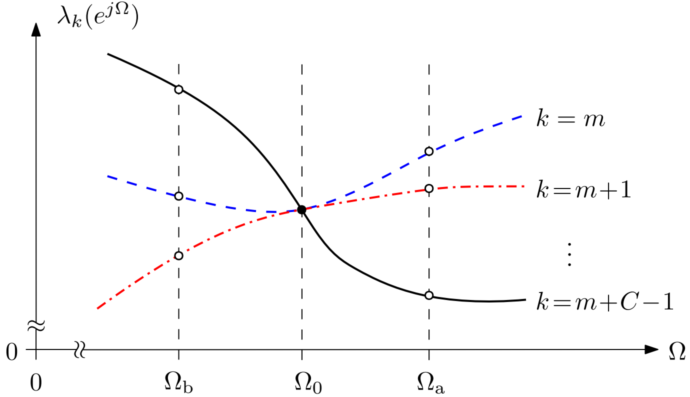


- maximally smooth continuation: analytic case . . . same as before;
- spectrally majorised case: eigenvalues $\lambda_m(e^{j\Omega})$ can be shown to be Lipschitz (stronger than Hölder) and analytic eigenvalues $\gamma_m(z)$ exis s.t. $\gamma_m(z)|_{z=e^{j\Omega}} = \lambda_m(e^{j\Omega})$.

# Polynomial Approximation of Eigenvalues

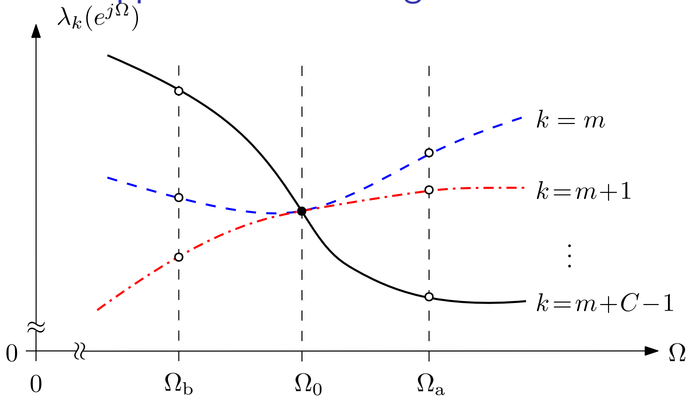


- Maximally smooth / analytic case will generally require a transcendental solution;
- for the spectrally majorised case, the convergence of the Laurent series will be slower;
- we expect to need a higher approximation order in case of spectral majorisation.

# Eigenvectors for Analytic Eigenvalues

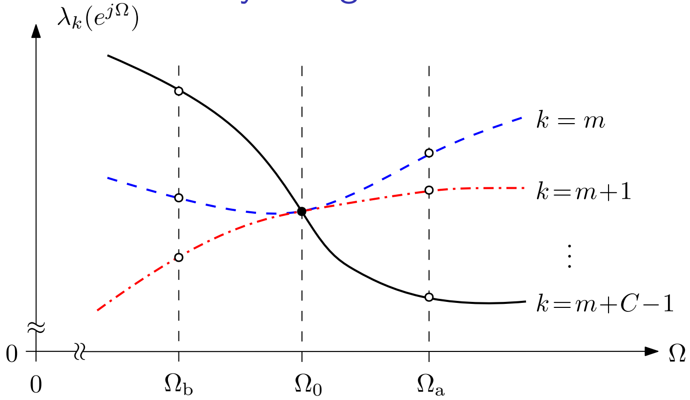


- For analytic eigenvalues, unique 1-d subspaces for the eigenvectors can be shown to continuous blend in and out of algebraic multiplicities;
- the existence of analytic eigenvectors $\mathbf{u}_m(z)$ again depends on the selection of the phase response within each subspace.

# Eigenvectors for Spectrally Majorised Eigenvalues

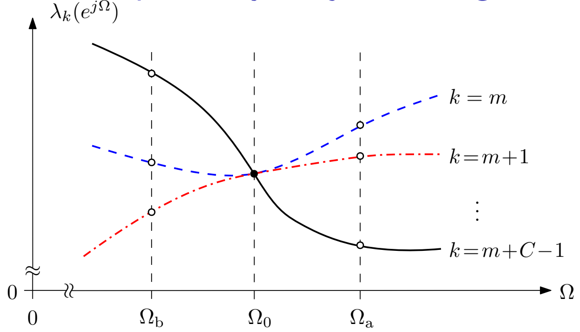


- For spectrally majorised eigenvalues, eigenvectors are discontinuous in the algebraic multiplicity;
- hence no exact analytic eigenvectors $\boldsymbol{u}_m(z)$ exist in this case, irrespective of the phase response;
- a Fourier series representation can be found if $\boldsymbol{q}_m(e^{j\Omega})$ has only a finite number of discontinuities;
- the series is not analytic, but a truncation can be.

# Numerical Example

University of Strathclyde Engineering

- We take a parahermitian matrix with known factors:

$$\boldsymbol{\Gamma}(z) = \begin{bmatrix} z+3+z^{-1} & \\ & -jz+3+jz^{-1} \end{bmatrix}$$

$$\boldsymbol{U}(z) = [\boldsymbol{u}_1(z),\, \boldsymbol{u}_2(z)] \qquad \text{with} \qquad \boldsymbol{u}_{1,2}(z) = \frac{1}{\sqrt{2}} \begin{bmatrix} 1 \\ \pm z^{-1} \end{bmatrix} ;$$

- parahermitian matrix $\boldsymbol{R}(z) = \boldsymbol{U}(z)\boldsymbol{\Gamma}(z)\boldsymbol{U}^{\mathrm{P}}(z)$:

$$\boldsymbol{R}(z) = \begin{bmatrix} \frac{1-j}{2}z+3+\frac{1+j}{2}z^{-1} & \frac{1+j}{2}z^{2}+\frac{1-j}{2} \\ \frac{1+j}{2}+\frac{1-j}{2}z^{-2} & \frac{1-j}{2}z+3+\frac{1+j}{2}z^{-1} \end{bmatrix} .$$

# Example — Maximally Smooth Case

- The factors represent the solution for the analytic eigenvalues and eigenvectors;

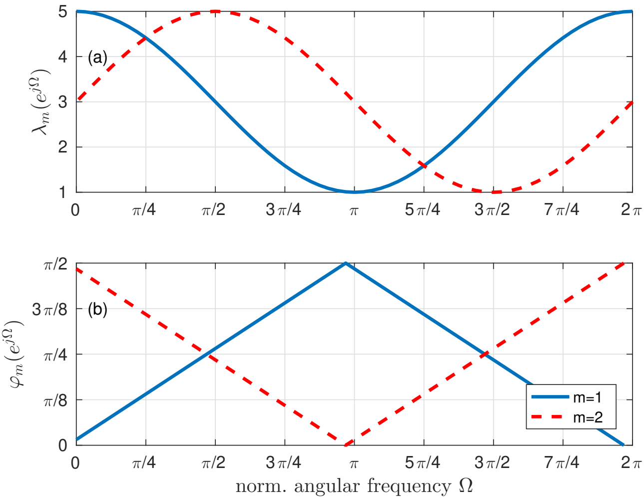

# Example — Spectral Majorisation

- On the unit circle, we end up with piecewise smooth eigenvalues and piecewith continuous eigenvectors — analytic solution only for the former [108, 105, 107]

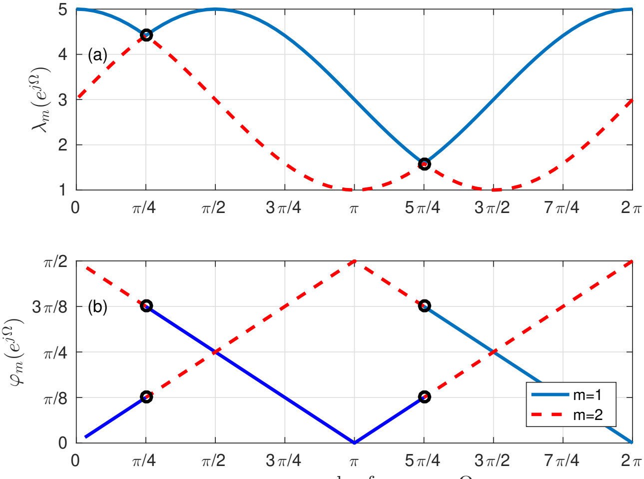

# Example — Algorithmic Solution

- Using an algorithm to approximate the McWhirter factorisation (order 24 for $\hat{\mathbf{\Gamma}}(z)$ and order 84 for $\hat{\boldsymbol{U}}(z)$) [58, 76, 81, 79, 22, 20, 95]:

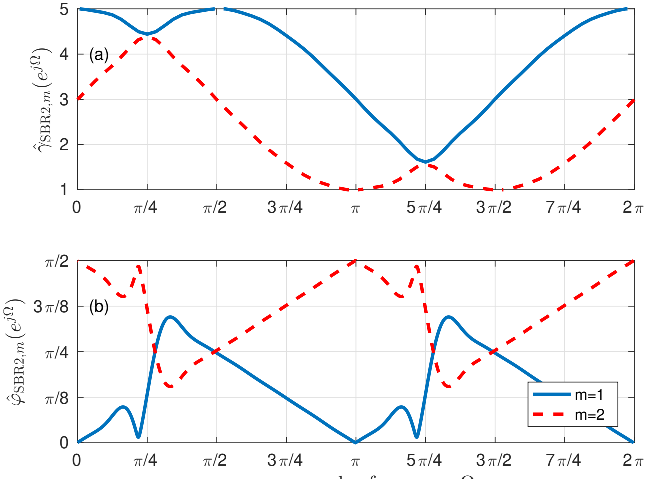

# McWhirter Decomposition

- John McWhirter et al. (2007): polynomial eigenvalue decomposition of a parahermitian matrix:

$$\boldsymbol{R}(z) \approx \boldsymbol{Q}(z)\boldsymbol{\Lambda}(z)\boldsymbol{Q}^{\mathrm{P}}(z)$$

- paraunitary (i.e. lossless) matrix $\boldsymbol{Q}(z)$, s.t. $\boldsymbol{Q}(z)\boldsymbol{Q}^{\mathrm{P}}(z) = \mathbf{I}$;
- diagonal and spectrally majorised $\boldsymbol{\Lambda}(z)$:

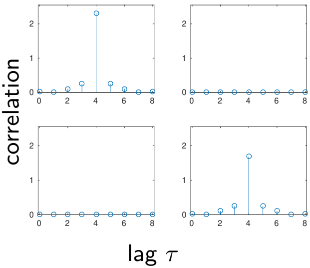


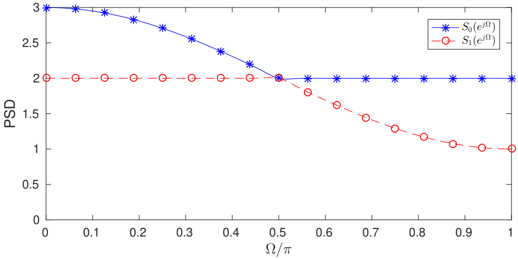

# Parahermitian Matrix EVD (PEVD)

- Franz Rellich (1937): for $\boldsymbol{R}(e^{j\Omega})$ analytic, there exist analytic eigenvectors $\boldsymbol{\Gamma}(e^{j\Omega})$ and analytic eigenvalues $\boldsymbol{U}(e^{j\Omega})$;
- can be generalised to

$$\boldsymbol{R}(z) = \boldsymbol{U}(z)\boldsymbol{\Gamma}(z)\boldsymbol{U}^{\mathrm{P}}(z) \; ;$$

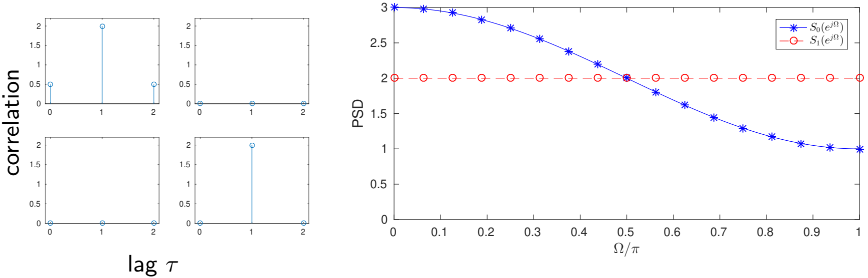


- eigenvalues are unique, eigenvectors can be modified by arbitrary allpass filters $H(z)$ (s.t. $H(z)H^{\mathrm{P}}(z) = 1$),

$$\boldsymbol{R}(z)\boldsymbol{u}(z)H(z) = \gamma(z)\boldsymbol{u}(z)H(z) \; .$$

# Further Reading

- For the existence and uniqueness of analytic eigenvalues and eigenvectors, please see [104, 103]
- McWhirter decomposition [57, 58].

# Iterative PEVD Algorithms

- Second order sequential best rotation (SBR2, McWhirter 2007);
- iterative approach based on an elementary paraunitary operation:

$$\begin{aligned} \boldsymbol{S}^{(0)}(z) &= \boldsymbol{R}(z) \\ &\vdots \\ \boldsymbol{S}^{(i+1)}(z) &= \tilde{\boldsymbol{H}}^{(i+1)}(z)\boldsymbol{S}^{(i)}(z)\boldsymbol{H}^{(i+1)}(z) \end{aligned}$$

- $\boldsymbol{H}^{(i)}(z)$ is an elementary paraunitary operation, which at the $i$th step eliminates the largest off-diagonal element in $\boldsymbol{s}^{(i-1)}(z)$;
- stop after $L$ iterations:

$$\hat{\boldsymbol{\Lambda}}(z) = \boldsymbol{S}^{(L)}(z) \qquad , \qquad \boldsymbol{Q}(z) = \prod_{i=1}^{L} \boldsymbol{H}^{(i)}(z)$$

- sequential matrix diagonalisation (SMD) and
- multiple-shift SMD (MS-SMD) will follow the same scheme ...

# Elementary Paraunitary Operation



- An elementary paraunitary matrix [Vaidyanathan] is defined as

$$\boldsymbol{H}^{(i)}(z) = \mathbf{I} - \mathbf{v}^{(i)}\mathbf{v}^{(i),\mathrm{H}} + z^{-1}\mathbf{v}^{(i)}\mathbf{v}^{(i),\mathrm{H}} \qquad , \quad \|\mathbf{v}^{(i)}\|_2 = 1$$

- we utilise a different definition:

$$\boldsymbol{H}^{(i)}(z) = \boldsymbol{D}^{(i)}(z)\mathbf{Q}^{(i)}$$

- $\boldsymbol{D}^{(i)}(z)$ is a delay matrix:

$$\boldsymbol{D}^{(i)}(z) = \mathrm{diag}\{1 \ \ldots \ 1 \ z^{-\tau} \ 1 \ \ldots \ 1\}$$

- $\mathbf{Q}^{(i)}(z)$ is a Givens rotation.

# Sequential Best Rotation Algorithm (McWhirter)

- At iteration $i$, consider $\boldsymbol{S}^{(i-1)}(z) \circ\!\!-\!\!\bullet\, \mathbf{S}^{(i-1)}[\tau]$

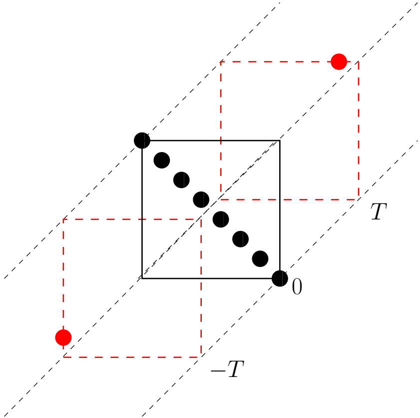

# Sequential Best Rotation Algorithm (McWhirter)

- $\tilde{\boldsymbol{D}}^{(i)}(z)\boldsymbol{S}^{(i-1)}(z)\boldsymbol{D}^{(i)}(z)$

$$\begin{bmatrix} 1 & & & \\ & \ddots & & \\ & & z^{T} & \\ & & & 1 \end{bmatrix} \cdot$$

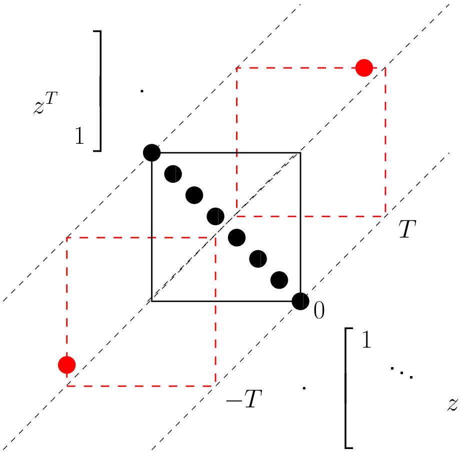


$$\cdot \begin{bmatrix} 1 & & & \\ & \ddots & & \\ & & z^{-T} & \\ & & & 1 \end{bmatrix}$$

# Sequential Best Rotation Algorithm (McWhirter)

- $\tilde{\boldsymbol{D}}^{(i)}(z)$ advances a row-slice of $\boldsymbol{S}^{(i-1)}(z)$ by $T$

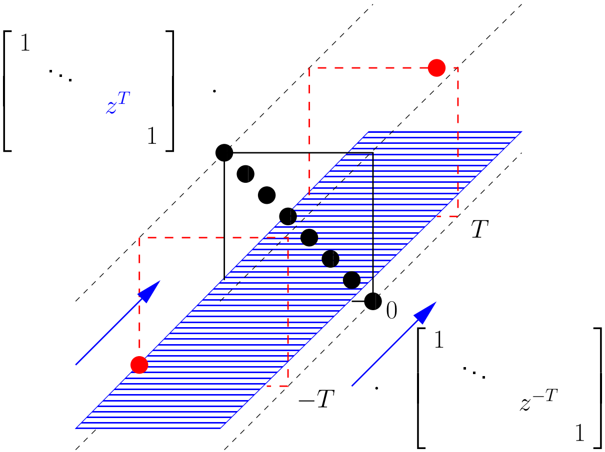

# Sequential Best Rotation Algorithm (McWhirter)

- the off-diagonal element at $-T$ has now been translated to lag zero

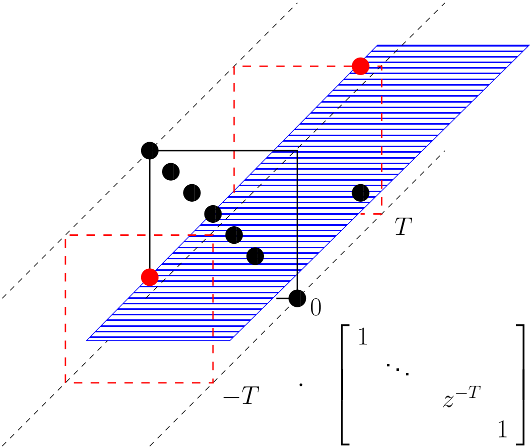


$$\cdot \begin{bmatrix} 1 & & & \\ & \ddots & & \\ & & z^{-T} & \\ & & & 1 \end{bmatrix}$$

# Sequential Best Rotation Algorithm (McWhirter)

- $\mathbf{D}^{(i)}(z)$ delays a column-slice of $\boldsymbol{S}^{(i-1)}(z)$ by $T$

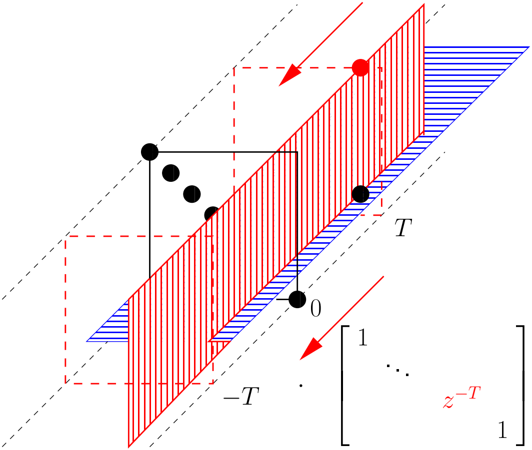

# Sequential Best Rotation Algorithm (McWhirter)

- the off-diagonal element at $-T$ has now been translated to lag zero

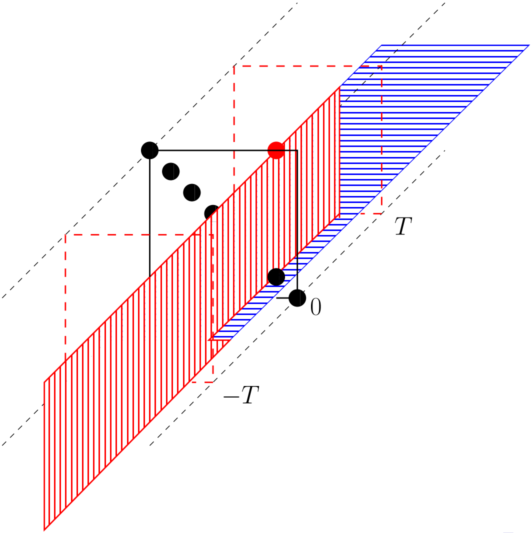

# Sequential Best Rotation Algorithm (McWhirter)

- the step $\tilde{\boldsymbol{D}}^{(i)}(z)\boldsymbol{S}^{(i-1)}(z)\boldsymbol{D}_{(i)}(z)$ has brought the largest off-diagonal elements to lag 0.

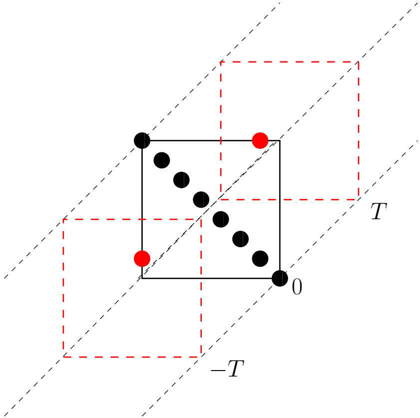

# Sequential Best Rotation Algorithm (McWhirter)

- Jacobi step to eliminate largest off-diagonal elements by $\mathbf{Q}^{(i)}$

$$\begin{bmatrix} c & & e^{-j\vartheta}s & \\ & \mathbf{I} & & \\ -e^{j\vartheta}s & & c & \\ & & & 1 \end{bmatrix} \cdot$$

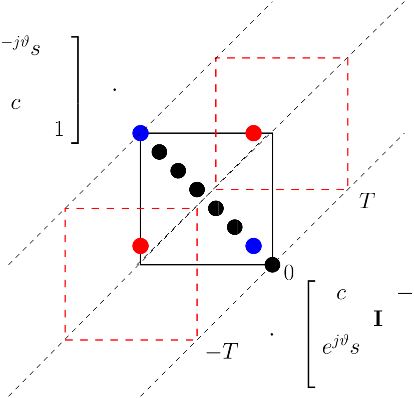


$$\cdot \begin{bmatrix} c & & -e^{-j\vartheta}s & \\ & \mathbf{I} & & \\ e^{j\vartheta}s & & c & \\ & & & 1 \end{bmatrix}$$

# Sequential Best Rotation Algorithm (McWhirter)

- iteration $i$ is completed, having performed

$$\boldsymbol{S}^{(i)}(z) = \mathbf{Q}^{(i)}\boldsymbol{D}^{(i)}(z)\boldsymbol{S}^{(i-1)}(z)\tilde{\boldsymbol{D}}^{(i)}(z)\tilde{\mathbf{Q}}^{(i)}(z)$$

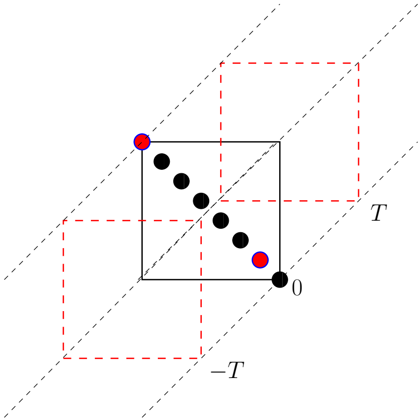

# SBR2 Outcome

- At the $i$th iteration, the zeroing of off-diagonal elements achieved during previous steps may be partially undone;
- however, the algorithm has been shown to converge, transfering energy onto the main diagonal at every step (McWhirter 2007);
- after $L$ iterations, we reach an approximate diagonalisation

$$\hat{\mathbf{\Lambda}}(z) = \boldsymbol{S}^{(L)}(z) = \tilde{\boldsymbol{Q}}(z)\boldsymbol{R}(z)\boldsymbol{Q}(z)$$

with

$$\boldsymbol{Q}(z) = \prod_{i=1}^{L} \boldsymbol{D}^{(i)}(z)\mathbf{Q}^{(i)}$$

- diagonalisation of the previous $3 \times 3$ polynomial matrix . . .

# SBR2 Example — Diagonalisation

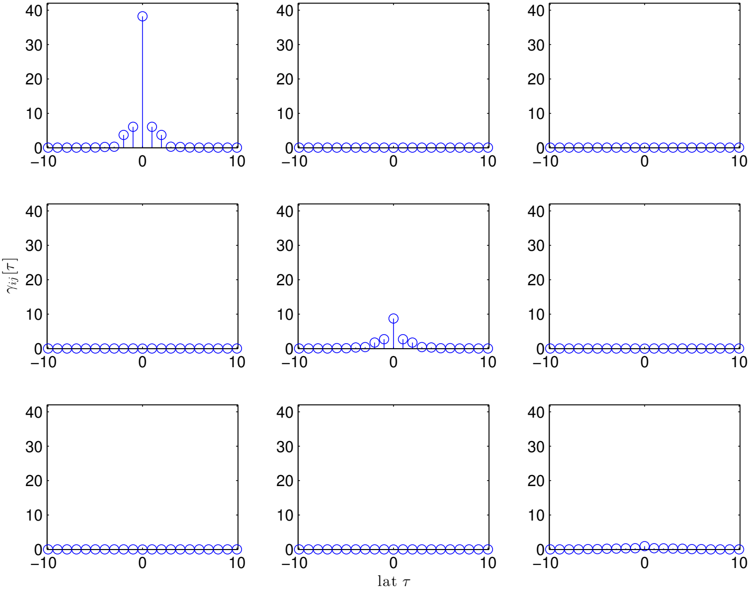


lag $\tau$

# SBR2 Example — Spectral Majorisation

- The on-diagonal elements are spectrally majorised

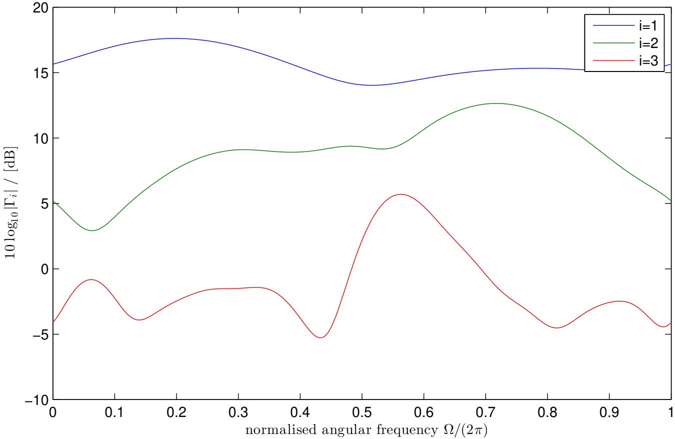

# SBR2 — Givens Rotation

- A Givens rotation eliminates the maximum off-diagonal element once brought onto the lag-zero matrix;
- note I: in the lag-zero matrix, one column and one row are modified by the shift:

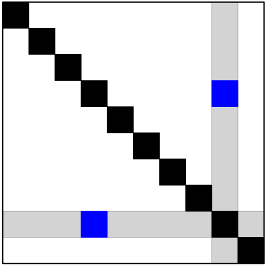

- note II: a Givens rotation only affects two columns and two rows in every matrix;
- Givens rotation is relatively low in computational cost!

# SBR2 — Givens Rotation

- A Givens rotation eliminates the maximum off-diagonal element once brought onto the lag-zero matrix;
- note I: in the lag-zero matrix, one column and one row are modified by the shift:

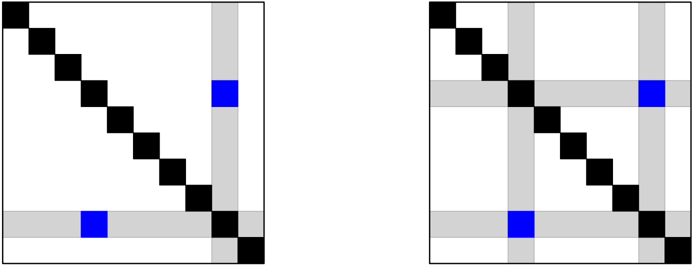

- note II: a Givens rotation only affects two columns and two rows in every matrix;
- Givens rotation is relatively low in computational cost!

# Sequential Matrix Diagonalisation (SMD)

(Redif *et al.*, IEEE Trans SP 2015, [79])

- Main idea — the zero-lag matrix is diagonalised in every step;
- initialisation: diagonalise $\mathbf{R}[0]$ by EVD and apply modal matrix to all matrix coefficients $\longrightarrow \boldsymbol{S}^{(0)}$;
- at the $i$th step as in SBR2, the maximum element (or column with max. norm) is shifted to the lag-zero matrix:

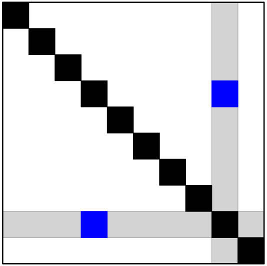

- an EVD is used to re-diagonalise the zero-lag matrix;
- a full modal matrix is applied at all lags — more costly than SBR2.

# Sequential Matrix Diagonalisation (SMD)

(Redif *et al.*, IEEE Trans SP 2015, [79])

- Main idea — the zero-lag matrix is diagonalised in every step;
- initialisation: diagonalise $\mathbf{R}[0]$ by EVD and apply modal matrix to all matrix coefficients $\longrightarrow \boldsymbol{S}^{(0)}$;
- at the $i$th step as in SBR2, the maximum element (or column with max. norm) is shifted to the lag-zero matrix:

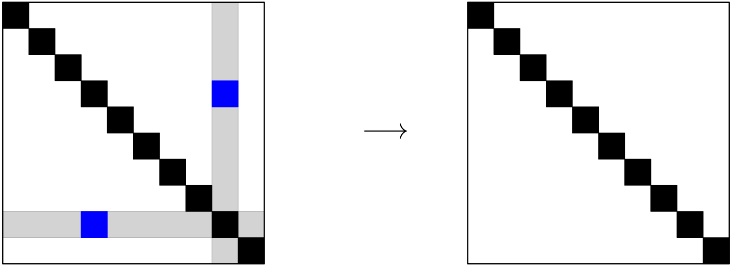

- an EVD is used to re-diagonalise the zero-lag matrix;
- a full modal matrix is applied at all lags — more costly than SBR2.

# Multiple Shift SMD (SMD)

- SMD converges faster than SBR2 — more energy is transfered per iteration step [22, 20, 25, 21];
- SMD is more expensive than SBR2 — full matrix multiplication at every lag;
- this cost will not increase further if more columns / rows are shifted into the lag-zero matrix at every iteration

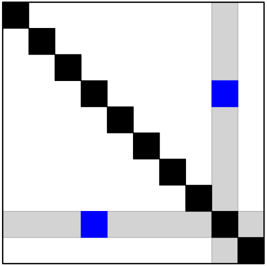

- MS-SMD will transfer yet more off-diagonal energy per iteration;
- because the total energy must remain constant under paraunitary operations, SBR2, SMD and MS-SMD can be proven to converge.

University of Strathclyde Engineering

# Multiple Shift SMD (SMD)

- SMD converges faster than SBR2 — more energy is transfered per iteration step [22, 20, 25, 21];
- SMD is more expensive than SBR2 — full matrix multiplication at every lag;
- this cost will not increase further if more columns / rows are shifted into the lag-zero matrix at every iteration

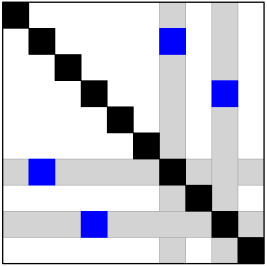

- MS-SMD will transfer yet more off-diagonal energy per iteration;
- because the total energy must remain constant under paraunitary operations, SBR2, SMD and MS-SMD can be proven to converge.

# Multiple Shift SMD (SMD)

- SMD converges faster than SBR2 — more energy is transfered per iteration step [22, 20, 25, 21];
- SMD is more expensive than SBR2 — full matrix multiplication at every lag;
- this cost will not increase further if more columns / rows are shifted into the lag-zero matrix at every iteration

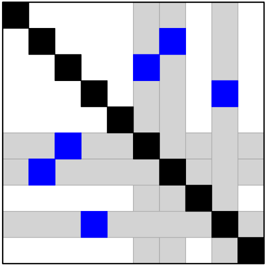

- MS-SMD will transfer yet more off-diagonal energy per iteration;
- because the total energy must remain constant under paraunitary operations, SBR2, SMD and MS-SMD can be proven to converge.

# Multiple Shift SMD (SMD)

- SMD converges faster than SBR2 — more energy is transfered per iteration step [22, 20, 25, 21];
- SMD is more expensive than SBR2 — full matrix multiplication at every lag;
- this cost will not increase further if more columns / rows are shifted into the lag-zero matrix at every iteration

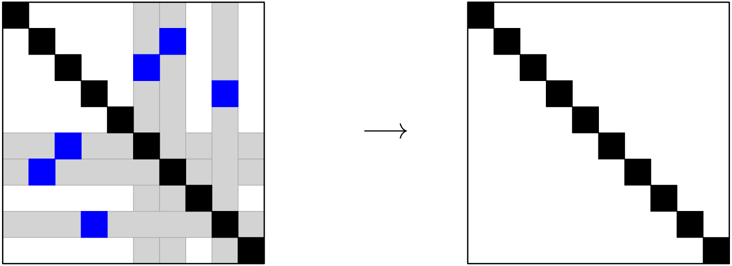

- MS-SMD will transfer yet more off-diagonal energy per iteration;
- because the total energy must remain constant under paraunitary operations, SBR2, SMD and MS-SMD can be proven to converge.

# SBR2/SMD/MS-SMD Convergence

- Measuring the remaining normalised off-diagonal energy over an ensemble of space-time covariance matrices:

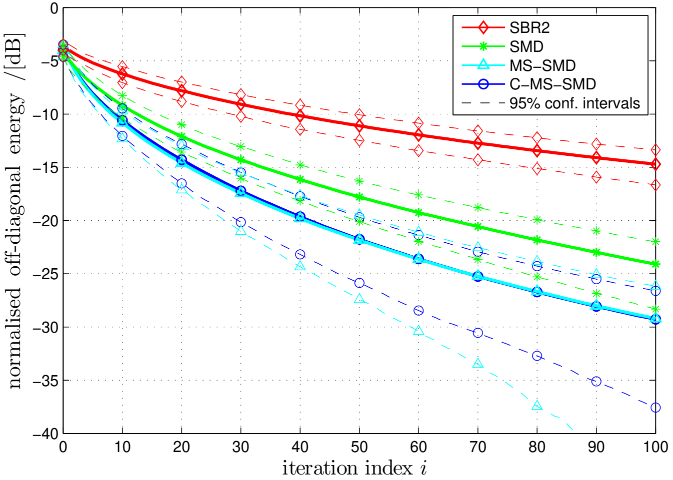

# SBR2/SMD/MS-SMD Application Cost 1

- Ensemble average of remaining off-diagonal energy vs. order of paraunitary filter banks to decompose 4x4x16 matrices:

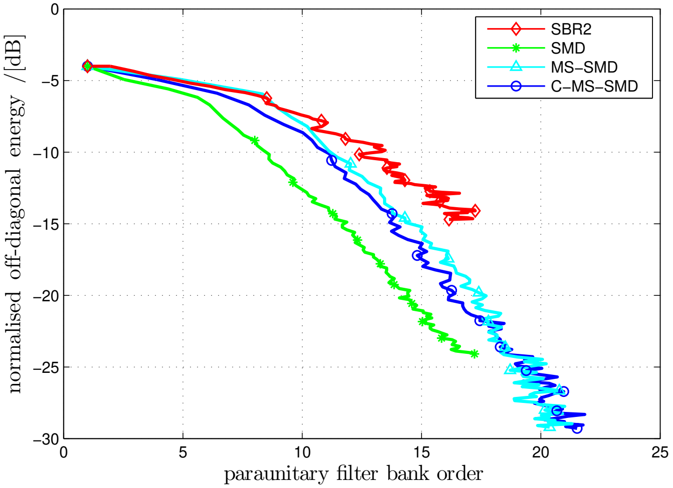

# SBR2/SMD/MS-SMD Application Cost 2

- Ensemble average of remaining off-diagonal energy vs. order of paraunitary filter banks to decompose 8x8x64 matrices:

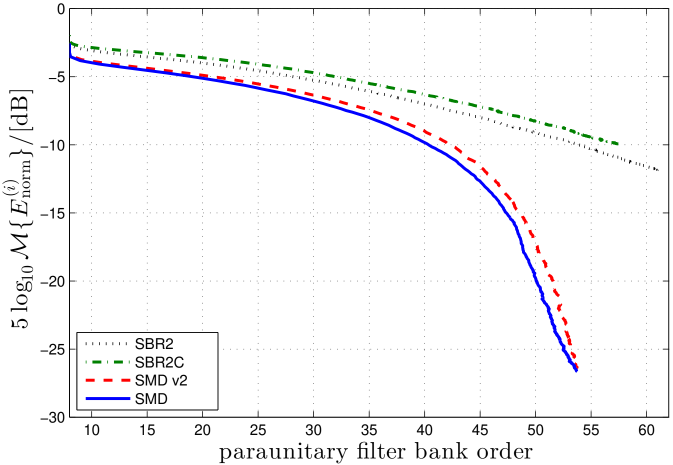

# Further Reading

- second order sequential best rotation (SBR2) algorithm [58];
- the SBR2 family of algorithms includes various modifications, such as to the cost function to maximise the coding gain: [76, 81]; multiple shift SBR2 [95, 94]; efficient implementation [49, 50];
- sequential matrix diagonalisation (SMD) algorithm [79], and various SMD family versions to undertake multiple shifts [22, 23, 20], apply search space reduction [25, 21, 30, 31], numerical efficiences [90, 19, 26, 27, 34, 37, 28, 33, 35]; a Householder approach to SMD [75];
- DFT domain algorithms to extract analytic solution — separate extraction of eigenvalues [108, 107] and eigenvectors [105] based on smoothness criteria [102, 109, 111]; a similar attempt had been undertaken in [91] with analysis in [32, 36];
- not shown here, but similar algorithms have been applied to other linear algebraic operations such as the QR decomposition [43, 44, 29] and the generalised EVD [18].

# MATLAB Polynomial EVD Toolbox

- The MATLAB polynomial EVD toolbox can be downloaded from

  `pevd-toolbox.eee.strath.ac.uk`

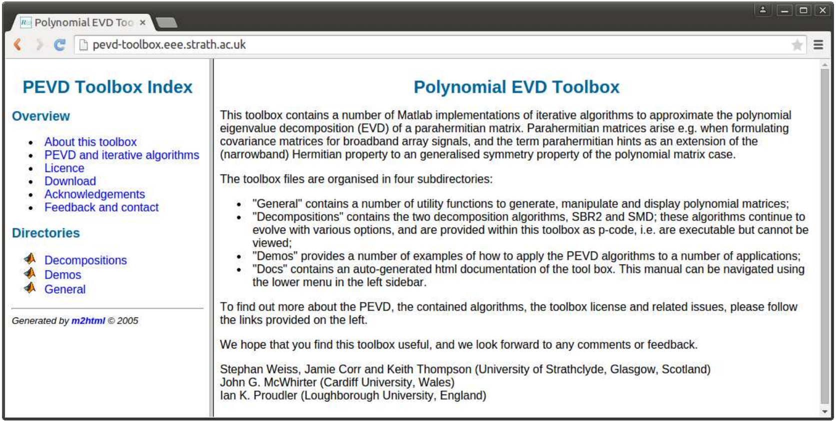

Polynomial EVD Too ×

pevd-toolbox.eee.strath.ac.uk

## PEVD Toolbox Index

### Overview

- About this toolbox
- PEVD and iterative algorithms
- Licence
- Download
- Acknowledgements
- Feedback and contact

### Directories

- Decompositions
- Demos
- General

*Generated by* ***m2html*** *© 2005*

## Polynomial EVD Toolbox

This toolbox contains a number of Matlab implementations of iterative algorithms to approximate the polynomial eigenvalue decomposition (EVD) of a parahermitian matrix. Parahermitian matrices arise e.g. when formulating covariance matrices for broadband array signals, and the term parahermitian hints as an extension of the (narrowband) Hermitian property to an generalised symmetry property of the polynomial matrix case.

The toolbox files are organised in four subdirectories:

- "General" contains a number of utility functions to generate, manipulate and display polynomial matrices;
- "Decompositions" contains the two decomposition algorithms, SBR2 and SMD; these algorithms continue to evolve with various options, and are provided within this toolbox as p-code, i.e. are executable but cannot be viewed;
- "Demos" provides a number of examples of how to apply the PEVD algorithms to a number of applications;
- "Docs" contains an auto-generated html documentation of the tool box. This manual can be navigated using the lower menu in the left sidebar.

To find out more about the PEVD, the contained algorithms, the toolbox license and related issues, please follow the links provided on the left.

We hope that you find this toolbox useful, and we look forward to any comments or feedback.

Stephan Weiss, Jamie Corr and Keith Thompson (University of Strathclyde, Glasgow, Scotland)
John G. McWhirter (Cardiff University, Wales)
Ian K. Proudler (Loughborough University, England)

- the toolbox contains a number of iterative algorithms to calculate an approximate PEVD, related functions, and demos.

# Narrowband MIMO Communications

- a narrowband channel is characterised by a matrix $\mathbf{C}$ containing complex gain factors;
- problem: how to select the precoder and equaliser?

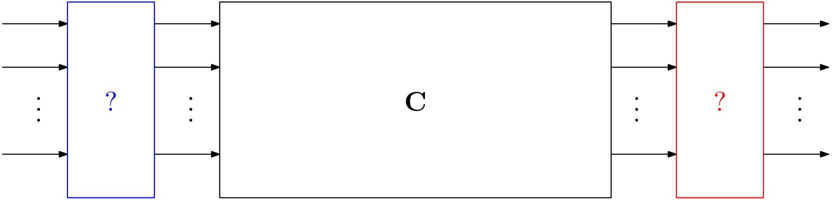


- overall system;

# Narrowband MIMO Communications

- a narrowband channel is characterised by a matrix $\mathbf{C}$ containing complex gain factors;
- problem: how to select the precoder and equaliser?

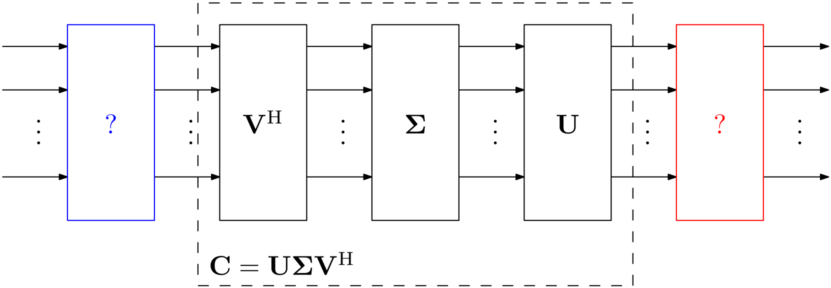


- the singular value decomposition (SVD) factorises $\mathbf{C}$ into two unitary matrices $\mathrm{U}$ and $\mathbf{V}^{\mathrm{H}}$ and a diagonal matrix $\boldsymbol{\Sigma}$;

# Narrowband MIMO Communications

- a narrowband channel is characterised by a matrix $\mathbf{C}$ containing complex gain factors;
- problem: how to select the precoder and equaliser?

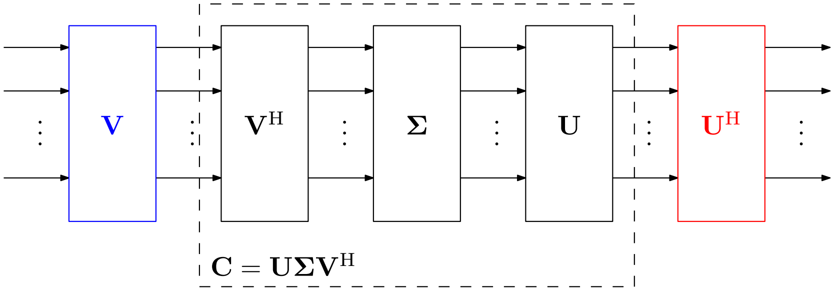


- we select the precoder and the equaliser from the unitary matrices provided by the channel's SVD;
- the overall system is diagonalised, decoupling the channel into independent single-input single-output systems by means of unitary matrices.

# Broadband MIMO Channel

- The channel is now a matrix of FIR filters; example for a $3 \times 4$ MIMO system $\mathbf{C}[n]$:

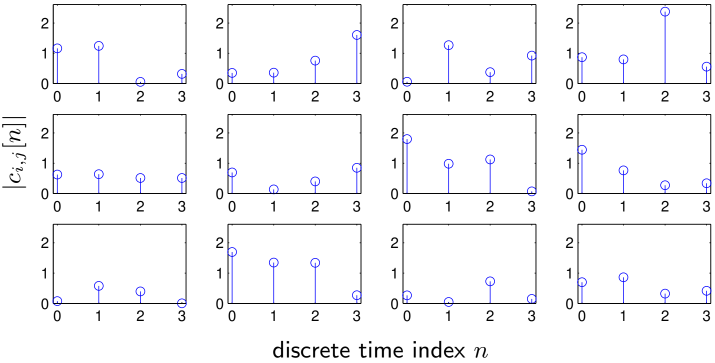


- the transfer function $\boldsymbol{C}(z) \bullet\!\!-\!\!\circ\, \mathbf{C}[n]$ is a polynomial matrix;
- an SVD can only diagonalise $\mathbf{C}[n]$ for one particular lag $n$.

# Standard Broadband MIMO Approaches

- OFDM (if approximate channel length is known):
  1. divide spectrum into narrowband channels;
  2. address each narrowband channel independently using narrowband-optimal techniques;

  drawback: ignores spectral coherence across frequency bins;
- optimum filter bank transceiver (if channel itself is known):
  1. block processing;
  2. inter-block interference is eliminated by guard intervals;
  3. resulting matrix can be diagonalised by SVD;
- both techniques invest DOFs into the guard intervals, which are generally not balanced against other error sources.

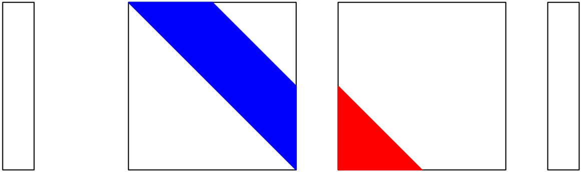

$$\mathbf{y}(z) = \left( \mathbf{C}_0 + \mathbf{C}_1 z^{-1} \right) \cdot \mathbf{x}(z)$$

# Standard Broadband MIMO Approaches

- OFDM (if approximate channel length is known):
  1. divide spectrum into narrowband channels;
  2. address each narrowband channel independently using narrowband-optimal techniques;

  drawback: ignores spectral coherence across frequency bins;
- optimum filter bank transceiver (if channel itself is known):
  1. block processing;
  2. inter-block interference is eliminated by guard intervals;
  3. resulting matrix can be diagonalised by SVD;
- both techniques invest DOFs into the guard intervals, which are generally not balanced against other error sources.

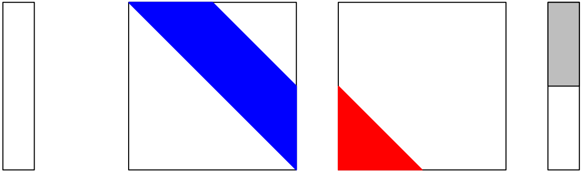

$$\mathbf{y}(z) = \left( \mathbf{C}_0 + \mathbf{C}_1 z^{-1} \right) \cdot \mathbf{x}(z)$$

# Standard Broadband MIMO Approaches

- OFDM (if approximate channel length is known):
  1. divide spectrum into narrowband channels;
  2. address each narrowband channel independently using narrowband-optimal techniques;

  drawback: ignores spectral coherence across frequency bins;
- optimum filter bank transceiver (if channel itself is known):
  1. block processing;
  2. inter-block interference is eliminated by guard intervals;
  3. resulting matrix can be diagonalised by SVD;
- both techniques invest DOFs into the guard intervals, which are generally not balanced against other error sources.

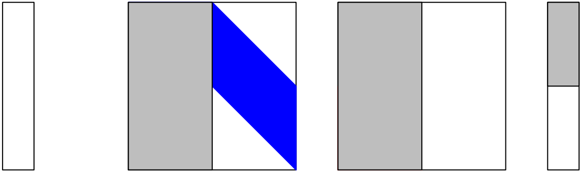

$$\mathbf{y}(z) = \Big( \quad \mathbf{C}'_0 \quad \Big) \cdot \mathbf{x}(z)$$

# Standard Broadband MIMO Approaches

- OFDM (if approximate channel length is known):
  1. divide spectrum into narrowband channels;
  2. address each narrowband channel independently using narrowband-optimal techniques;

  drawback: ignores spectral coherence across frequency bins;
- optimum filter bank transceiver (if channel itself is known):
  1. block processing;
  2. inter-block interference is eliminated by guard intervals;
  3. resulting matrix can be diagonalised by SVD;
- both techniques invest DOFs into the guard intervals, which are generally not balanced against other error sources.

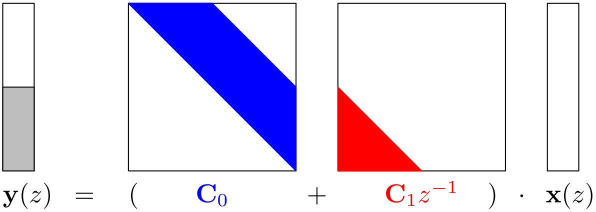

# Standard Broadband MIMO Approaches

- OFDM (if approximate channel length is known):
  1. divide spectrum into narrowband channels;
  2. address each narrowband channel independently using narrowband-optimal techniques;

  drawback: ignores spectral coherence across frequency bins;
- optimum filter bank transceiver (if channel itself is known):
  1. block processing;
  2. inter-block interference is eliminated by guard intervals;
  3. resulting matrix can be diagonalised by SVD;
- both techniques invest DOFs into the guard intervals, which are generally not balanced against other error sources.

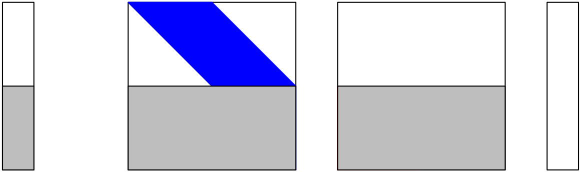

$$\mathbf{y}(z) = ( \quad \mathbf{C}_0' \quad ) \cdot \mathbf{x}(z)$$

# Polynomial Singular Value Decompositions

- Iterative algorithms have been developed to determine a polynomial eigenvalue decomposition (EVD) for a parahermitian matrix $\boldsymbol{R}(z) = \boldsymbol{R}^{\mathrm{P}}(z) = \boldsymbol{R}^{\mathrm{H}}(z^{-1})$:

$$\boldsymbol{R}(z) \approx \boldsymbol{H}(z)\boldsymbol{\Gamma}(z)\boldsymbol{H}^{\mathrm{P}}(z)$$

- paraunitary $\boldsymbol{H}(z)\boldsymbol{H}^{\mathrm{P}}(z) = \mathbf{I}$, diagonal and spectrally majorised $\boldsymbol{\Gamma}(z)$;
- polynomial SVD of channel $\boldsymbol{C}(z)$ can be obtained via two EVDs:

$$\boldsymbol{C}(z)\tilde{\boldsymbol{C}}(z) = \boldsymbol{U}(z)\boldsymbol{\Sigma}^{+}(z)\boldsymbol{\Sigma}^{-}(z)\boldsymbol{U}^{\mathrm{P}}(z)$$
$$\tilde{\boldsymbol{C}}(z)\boldsymbol{C}(z) = \boldsymbol{V}(z)\boldsymbol{\Sigma}^{-}(z)\boldsymbol{\Sigma}^{+}(z)\boldsymbol{V}^{\mathrm{P}}(z)$$

finally:

$$\boldsymbol{C}(z) = \boldsymbol{U}(z)\boldsymbol{\Sigma}^{+}(z)\boldsymbol{V}^{\mathrm{P}}(z)$$

University of Strathclyde Engineering

# MIMO Application Example

- Polynomial SVD of the previous $\boldsymbol{C}(z) \in \mathbb{C}^{3\times 4}$ channel matrix:

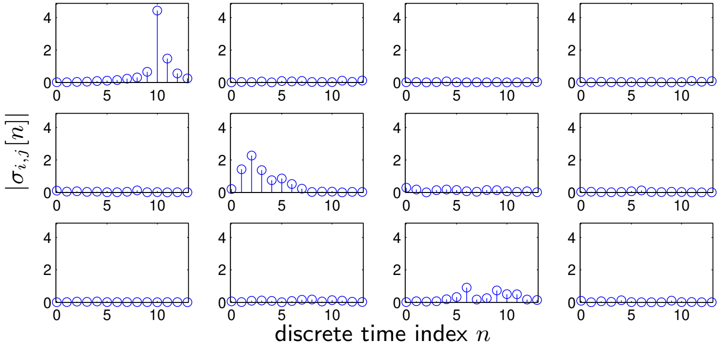


- the singular value spectra are majorised:

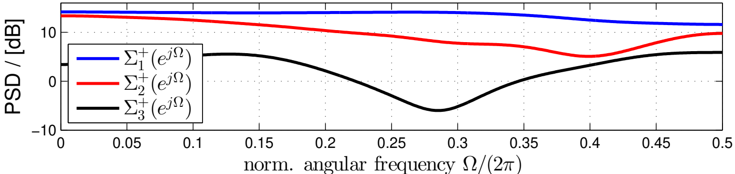

# Further Reading

- General precoding and equalisation [86, 89, 87, 88, 55, 54, 85, 2, 68];
- joint source-channel coding [97, 96, 110];
- subband coding [77, 76, 81];
- polynomial Wiener filter as optimum receiver [56, 53, 112]
- non-linear precoding for broadband MIMO systems [1, 4, 3, 61, 62, 5, 7, 6, 8, 64, 66, 63, 65, 67, 59, 60];
- combination with filter bank multicarrier methods [113, 69, 70, 71, 17];
- related using a polynomial generalised SVD [47].

# Narrowband Source Model

University of Strathclyde Engineering

- Scenario with sensor array and far-field sources:

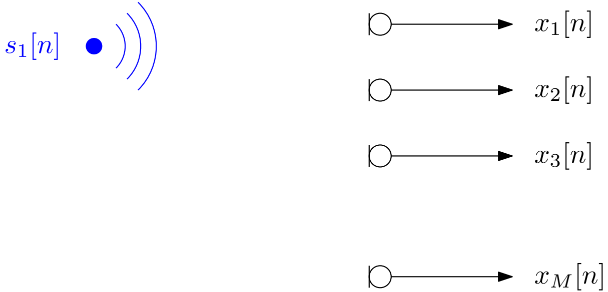


- for the narrowband case, the source signals arrive with delays, expressed by phase shifts in a steering vector
- data model:

$$\mathbf{x}[n] =$$

# Narrowband Source Model

- Scenario with sensor array and far-field sources:

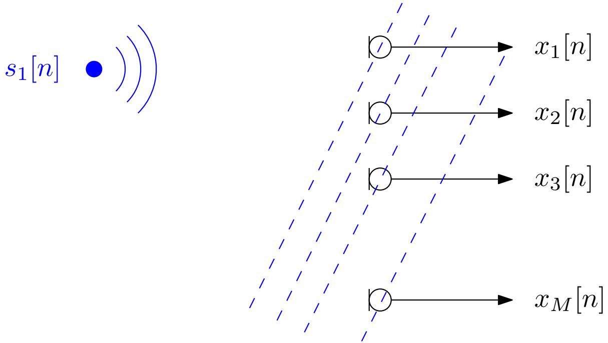


- for the narrowband case, the source signals arrive with delays, expressed by phase shifts in a steering vector $\mathbf{s}_1$
- data model:

$$\mathbf{x}[n] = s_1[n] \cdot \mathbf{s}_1$$

# Narrowband Source Model

- Scenario with sensor array and far-field sources:

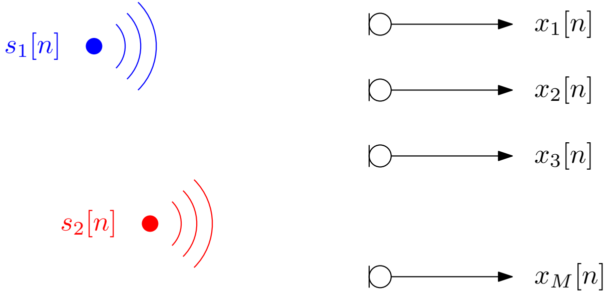


- for the narrowband case, the source signals arrive with delays, expressed by phase shifts in a steering vector $\mathbf{s}_1$
- data model:

$$\mathbf{x}[n] = s_1[n] \cdot \mathbf{s}_1$$

# Narrowband Source Model

- Scenario with sensor array and far-field sources:

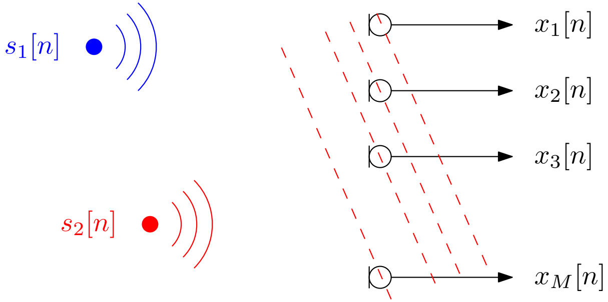


- for the narrowband case, the source signals arrive with delays, expressed by phase shifts in a steering vector $\mathbf{s}_1$, $\mathbf{s}_2$
- data model:

$$\mathbf{x}[n] = s_1[n] \cdot \mathbf{s}_1 + s_1[n] \cdot \mathbf{s_2}$$

# Narrowband Source Model

- Scenario with sensor array and far-field sources:

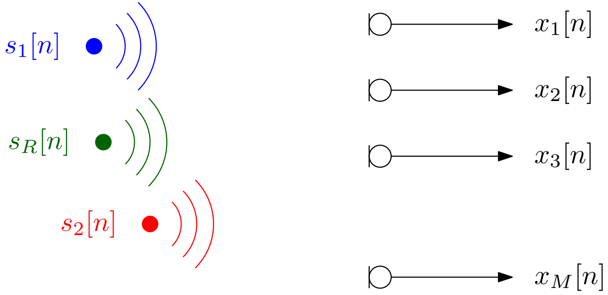


- for the narrowband case, the source signals arrive with delays, expressed by phase shifts in a steering vector $\mathbf{s}_1$, $\mathbf{s}_2$
- data model:

$$\mathbf{x}[n] = s_1[n] \cdot \mathbf{s}_1 + s_1[n] \cdot \mathbf{s_2}$$

# Narrowband Source Model

- Scenario with sensor array and far-field sources:

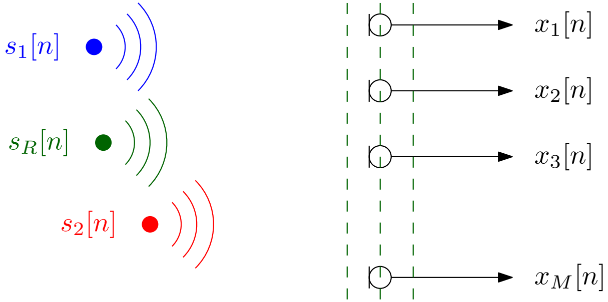


- for the narrowband case, the source signals arrive with delays, expressed by phase shifts in a steering vector $\mathbf{s}_1$, $\mathbf{s}_2$, $\ldots \mathbf{s}_R$;
- data model:

$$\mathbf{x}[n] = s_1[n] \cdot \mathbf{s}_1 + s_1[n] \cdot \mathbf{s_2} + \cdots + s_R[n] \cdot \mathbf{s}_R = \sum_{r=1}^{R} s_r[n] \cdot \mathbf{s}_r$$

# Steering Vector

- A signal $s[n]$ arriving at the array can be characterised by the delays of its wavefront (neglecting attenuation):

$$\begin{bmatrix} x_0[n] \\ x_1[n] \\ \vdots \\ x_{M-1}[n] \end{bmatrix} = \begin{bmatrix} s[n-\tau_0] \\ s[n-\tau_1] \\ \vdots \\ s[n-\tau_{M-1}] \end{bmatrix} = \begin{bmatrix} \delta[n-\tau_0] \\ \delta[n-\tau_1] \\ \vdots \\ \delta[n-\tau_{M-1}] \end{bmatrix} * s[n] \circ\!\!-\!\!\bullet\ \mathbf{a}_\vartheta(z)S(z)$$

- if evaluated at a narrowband normalised angular frequency $\Omega_i$, the time delays $\tau_m$ in the broadband steering vector $\mathbf{a}_\vartheta(z)$ collapse to phase shifts in the narrowband steering vector $\mathbf{a}_{\vartheta,\Omega_i}$,

$$\mathbf{a}_{\vartheta,\Omega_i} = \mathbf{a}_\vartheta(z)|_{z=e^{j\Omega_i}} = \begin{bmatrix} e^{-j\tau_0\Omega_i} \\ e^{-j\tau_1\Omega_i} \\ \vdots \\ e^{-j\tau_{M-1}\Omega_i} \end{bmatrix} .$$

# Data and Covariance Matrices

- A data matrix $\mathbf{X} \in \mathbb{C}^{M \times L}$ can be formed from $L$ measurements:

$$\mathbf{X} = \left[ \begin{array}{cccc} \mathbf{x}[n] & \mathbf{x}[n+1] & \dots & \mathbf{x}[n+L-1] \end{array} \right]$$

- assuming that all $x_m[n]$, $m = 1, 2, \dots M$ are zero mean, the (instantaneous) data covariance matrix is

$$\mathbf{R} = \mathcal{E}\{\mathbf{x}[n]\mathbf{x}^{\mathrm{H}}[n]\} \approx \frac{1}{L}\mathbf{X}\mathbf{X}^{\mathrm{H}}$$

  where the approximation assumes ergodicity and a sufficiently large $L$;
- Problem: can we tell from $\mathbf{X}$ or $\mathbf{R}$ (i) the number of sources and (ii) their orgin / time series?
- w.r.t. Jonathon Chamber's introduction, we here only consider the underdetermined case of more sensors than sources, $M \geq K$, and generally $L \gg M$.

# SVD of Data Matrix

- Singular value decomposition of $\mathbf{X}$:

$$\mathbf{X} = \mathbf{U} \; \boldsymbol{\Sigma} \; \mathbf{V}^{\mathrm{H}}$$

- unitary matrices $\mathbf{U} = [\mathbf{u}_1 \ldots \mathbf{u}_M]$ and $\mathbf{V} = [\mathbf{v}_1 \ldots \mathbf{v}_L]$;
- diagonal $\boldsymbol{\Sigma}$ contains the real, positive semidefinite singular values of $\mathbf{X}$ in descending order:

$$\boldsymbol{\Sigma} = \begin{bmatrix} \sigma_1 & 0 & \ldots & 0 & 0 & \ldots & 0 \\ 0 & \sigma_2 & \ddots & \vdots & \vdots & & \vdots \\ \vdots & \ddots & \ddots & 0 & \vdots & & \vdots \\ 0 & & 0 & \sigma_M & 0 & \ldots & 0 \end{bmatrix}$$

with $\sigma_1 \geq \sigma_2 \geq \cdots \geq \sigma_M \geq 0$.

# Singular Values

- If the array is illuminated by $R \leq M$ linearly independent sources, the rank of
  the data matrix is
  $$\text{rank}\{\mathbf{X}\} = R$$
- only the first $R$ singular values of $\mathbf{X}$ will be non-zero;
- in practice, noise often will ensure that $\text{rank}\{\mathbf{X}\} = M$, with $M - R$ trailing singular values that define the noise floor:

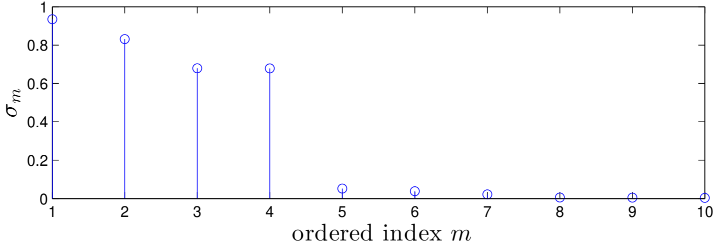


- therefore, by thresholding singular values, it is possible to estimate the number of linearly independent sources $R$.

University of Strathclyde Engineering

# Subspace Decomposition

- If rank$\{\mathbf{X}\} = R$, the SVD can be split:

$$\mathbf{X} = [\mathbf{U}_s \;\; \mathbf{U}_n] \begin{bmatrix} \boldsymbol{\Sigma}_s & \mathbf{0} \\ \mathbf{0} & \boldsymbol{\Sigma}_n \end{bmatrix} \begin{bmatrix} \mathbf{V}_s^{\mathrm{H}} \\ \mathbf{V}_n^{\mathrm{H}} \end{bmatrix}$$

- with $\mathbf{U}_s \in \mathbb{C}^{M\times R}$ and $\mathbf{V}_s^{\mathrm{H}} \in \mathbb{C}^{R\times L}$ corresponding to the $R$ largest singular values;
- $\mathbf{U}_s$ and $\mathbf{V}_s^{\mathrm{H}}$ define the signal-plus-noise subspace of $\mathbf{X}$:

$$\mathbf{X} = \sum_{m=1}^{M} \sigma_m \mathbf{u}_m \mathbf{v}_m^{\mathrm{H}} \approx \sum_{m=1}^{R} \sigma_m \mathbf{u}_m \mathbf{v}_m^{\mathrm{H}}$$

- the complements $\mathbf{U}_n$ and $\mathbf{V}_n^{\mathrm{H}}$,

$$\mathbf{U}_s^{\mathrm{H}}\mathbf{U}_n = \mathbf{0} \qquad , \qquad \mathbf{V}_s\mathbf{V}_n^{\mathrm{H}} = \mathbf{0}$$

define the noise-only subspace of $\mathbf{X}$.

# SVD via Two EVDs

- Any Hermitian matrix $\mathbf{A} = \mathbf{A}^{\rm H}$ allows an eigenvalue decomposition
$$\mathbf{A} = \mathbf{Q}\boldsymbol{\Lambda}\mathbf{Q}^{\rm H}$$
with $\mathbf{Q}$ unitary and the eigenvalues in $\boldsymbol{\Lambda}$ real valued and positive semi-definite;
- postulating $\mathbf{X} = \mathbf{U}\boldsymbol{\Sigma}\mathbf{V}^{\rm H}$, therefore:

$$\mathbf{X}\mathbf{X}^{\rm H} = (\mathbf{U}\boldsymbol{\Sigma}\mathbf{V}^{\rm H})(\mathbf{V}\boldsymbol{\Sigma}^{\rm H}\mathbf{U}^{\rm H}) = \mathbf{U}\boldsymbol{\Lambda}\mathbf{U}^{\rm H} \qquad (38)$$
$$\mathbf{X}^{\rm H}\mathbf{X} = (\mathbf{V}\boldsymbol{\Sigma}^{\rm H}\mathbf{U}^{\rm H})(\mathbf{U}\boldsymbol{\Sigma}\mathbf{V}^{\rm H}) = \mathbf{V}\boldsymbol{\Lambda}\mathbf{V}^{\rm H} \qquad (39)$$

- (ordered) eigenvalues relate to the singular values: $\lambda_m = \sigma_m^2$;
- the covariance matrix $\mathbf{R} = \frac{1}{L}\mathbf{X}\mathbf{X}$ has the same rank as the data matrix $\mathbf{X}$, and with $\mathbf{U}$ provides access to the same spatial subspace decomposition.

# Narrowband MUSIC Algorithm

- EVD of the narrowband covariance matrix identifies signal-plus-noise and noise-only subspaces

$$\mathbf{R} = [\mathbf{U}_s \;\; \mathbf{U}_n] \begin{bmatrix} \mathbf{\Lambda}_s & \mathbf{0} \\ \mathbf{0} & \mathbf{\Lambda}_n \end{bmatrix} \begin{bmatrix} \mathbf{U}_s^{\mathrm{H}} \\ \mathbf{U}_n^{\mathrm{H}} \end{bmatrix}$$

- scanning the signal-plus-noise subspace could only help to retrieve sources with orthogonal steering vectors;
- therefore, the multiple signal classification (MUSIC) algorithm scans the noise-only subspace for minima, or maxima of its reciprocal

$$S_{\mathrm{MUSIC}}(\vartheta) = \frac{1}{\|\mathbf{U}_n \mathbf{a}_{\vartheta,\Omega_i}\|_2^2}$$

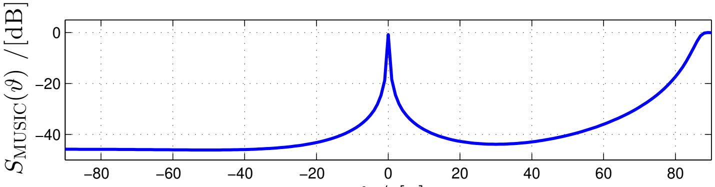

# Narrowband Source Separation

- Via SVD of the data matrix $\mathbf{X}$ or EVD of the covariance matrix $\mathbf{R}$, we can determine the number of linearly independent sources $R$;
- using the subspace decompositions offered by EVD/SVD, the directions of arrival can be estimated using e.g. MUSIC;
- based on knowledge of the angle of arrival, beamforming could be applied to $\mathbf{X}$ to extract specific sources;
- overall: EVD (and SVD) can play a vital part in narrowband source separation;
- what about broadband source separation?

# Broadband Array Scenario

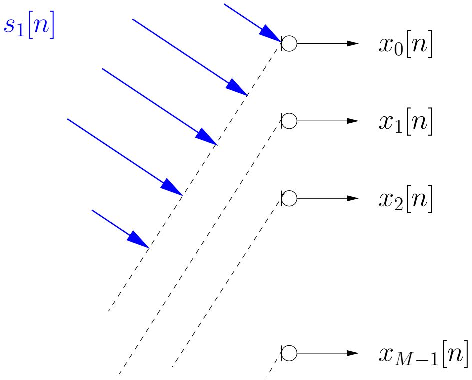


- Compared to the narrowband case, time delays rather than phase shifts bear information on the direction of a source.

# Broadband Steering Vector

- A signal $s[n]$ arriving at the array can be characterised by the delays of its wavefront (neglecting attenuation):

$$\begin{bmatrix} x_0[n] \\ x_1[n] \\ \vdots \\ x_{M-1}[n] \end{bmatrix} = \begin{bmatrix} s[n-\tau_0] \\ s[n-\tau_1] \\ \vdots \\ s[n-\tau_{M-1}] \end{bmatrix} = \begin{bmatrix} \delta[n-\tau_0] \\ \delta[n-\tau_1] \\ \vdots \\ \delta[n-\tau_{M-1}] \end{bmatrix} * s[n] \circ\!\!-\!\!\bullet\ \mathbf{a}_\vartheta(z)S(z)$$

- if evaluated at a narrowband normalised angular frequency $\Omega_i$, the time delays $\tau_m$ in the broadband steering vector $\mathbf{a}_\vartheta(z)$ collapse to phase shifts in the narrowband steering vector $\mathbf{a}_{\vartheta,\Omega_i}$,

$$\mathbf{a}_{\vartheta,\Omega_i} = \mathbf{a}_\vartheta(z)|_{z=e^{j\Omega_i}} = \begin{bmatrix} e^{-j\tau_0\Omega_i} \\ e^{-j\tau_1\Omega_i} \\ \vdots \\ e^{-j\tau_{M-1}\Omega_i} \end{bmatrix} .$$

# Space-Time Covariance Matrix

- If delays must be considered, the (space-time) covariance matrix must capture the lag $\tau$:

$$\mathbf{R}[\tau] = \mathcal{E}\{\mathbf{x}[n] \cdot \mathbf{x}^{\mathrm{H}}[n-\tau]\}$$

- $\mathbf{R}[\tau]$ contains auto- and cross-correlation sequences:

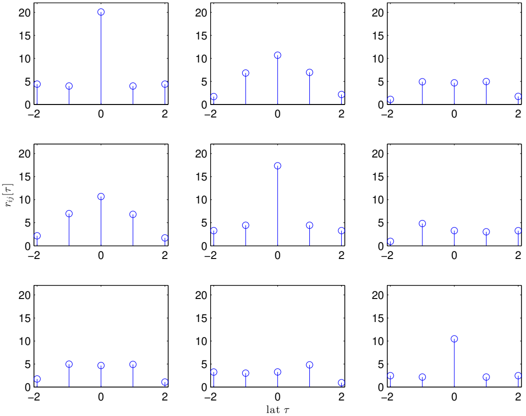

# Cross Spectral Density Matrix

- $z$-transform of the space-time covariance matrix is given by

$$\mathbf{R}[\tau] = \mathcal{E}\{\mathbf{x}_n \mathbf{x}^{\mathrm{H}}_{n-\tau}\} \quad \circ\!\!-\!\!\bullet \quad \boldsymbol{R}(z) = \sum_l S_l(z) \mathbf{a}_{\vartheta_l}(z) \mathbf{a}^{\mathrm{P}}_{\vartheta_l}(z) + \sigma^2_N \mathbf{I}$$

  with $\vartheta_l$ the direction of arrival and $S_l(z)$ the PSD of the $l$th source;
- $\boldsymbol{R}(z)$ is the cross spectral density (CSD) matrix;
- the instantaneous covariance matrix (no lag parameter $\tau$)

$$\mathbf{R} = \mathcal{E}\{\mathbf{x}_n \mathbf{x}^{\mathrm{H}}_n\} = \mathbf{R}[0]$$

# Polynomial MUSIC (PMUSIC)

[Alrmah, Weiss, Lambotharan, *EUSIPCO* (2011)]

- Based on the polynomial EVD of the broadband covariance matrix

$$\mathbf{R}(z) \approx \underbrace{[\mathbf{Q}_s(z) \;\; \mathbf{Q}_n(z)]}_{\mathbf{Q}(z)} \underbrace{\begin{bmatrix} \mathbf{\Lambda}_s(z) & \mathbf{0} \\ \mathbf{0} & \mathbf{\Lambda}_n(z) \end{bmatrix}}_{\mathbf{\Lambda}(z)} \begin{bmatrix} \mathbf{Q}_s^{\mathrm{P}}(z) \\ \mathbf{Q}_n^{\mathrm{P}}(z) \end{bmatrix}$$

- paraunitary $\mathbf{Q}(z)$, s.t. $\mathbf{Q}(z)\mathbf{Q}^{\mathrm{P}}(z) = \mathbf{I}$;
- diagonalised and spectrally majorised $\mathbf{\Lambda}(z)$:

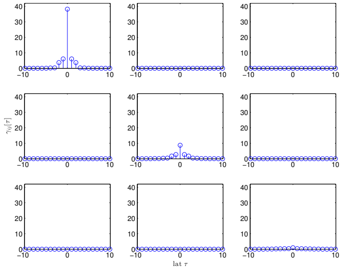


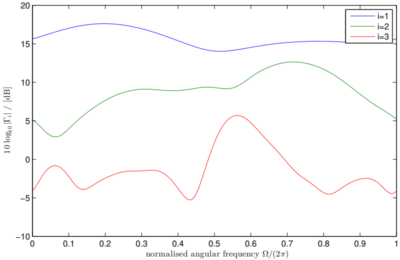

# PMUSIC cont'd

- Idea — scan the polynomial noise-only subspace $Q_n(z)$ with broadband steering vectors

$$\Gamma(z,\vartheta) = \mathbf{a}_{\vartheta}^{\mathrm{P}}(z)\mathbf{Q}_n^{\mathrm{P}}(z)\mathbf{Q}_n(z)\mathbf{a}_{\vartheta}(z)$$

- looking for minima leads to a spatio-spectral PMUSIC

$$S_{\mathrm{PSS-MUSIC}}(\vartheta,\Omega) = \left(\Gamma(z,\vartheta)|_{z=e^{j\Omega}}\right)^{-1}$$

- and a spatial-only PMUSIC

$$S_{\mathrm{PS-MUSIC}}(\vartheta) = \left(2\pi \oint \Gamma(z,\vartheta)|_{z=e^{j\Omega}} d\Omega\right)^{-1} = \Gamma_{\vartheta}^{-1}[0]$$

with $\Gamma_{\vartheta}[\tau] \circ\!\!-\!\!\bullet\, \Gamma(z,\vartheta)$.

# Simulation I — Toy Problem

- Linear uniform array with critical spatial and temporal sampling;
- broadband steering vector for end-fire position:

$$\mathbf{a}_{\pi/2}(z) = [1 \;\; z^{-1} \;\; \cdots \;\; z^{-M+1}]^{\mathrm{T}}$$

- covariance matrix

$$\mathbf{R}(z) = \mathbf{a}_{\pi/2}(z)\mathbf{a}^{\mathrm{P}}_{\pi/2}(z) = \begin{bmatrix} 1 & z^{1} & \ldots & z^{M-1} \\ z^{-1} & 1 & & \vdots \\ \vdots & & \ddots & \vdots \\ z^{-M+1} & \ldots & \ldots & 1 \end{bmatrix} .$$

- PEVD (by inspection)

$$\mathbf{Q}(z) = \mathbf{T}_{\mathrm{DFT}}\mathrm{diag}\left\{1 \;\; z^{-1} \;\; \cdots \;\; z^{-M+1}\right\} \quad ; \quad \mathbf{\Lambda}(z) = \mathrm{diag}\{1 \; 0 \; \cdots \; 0$$

- simulations with $M = 4$ ...

# Simulation I — PSS-MUSIC

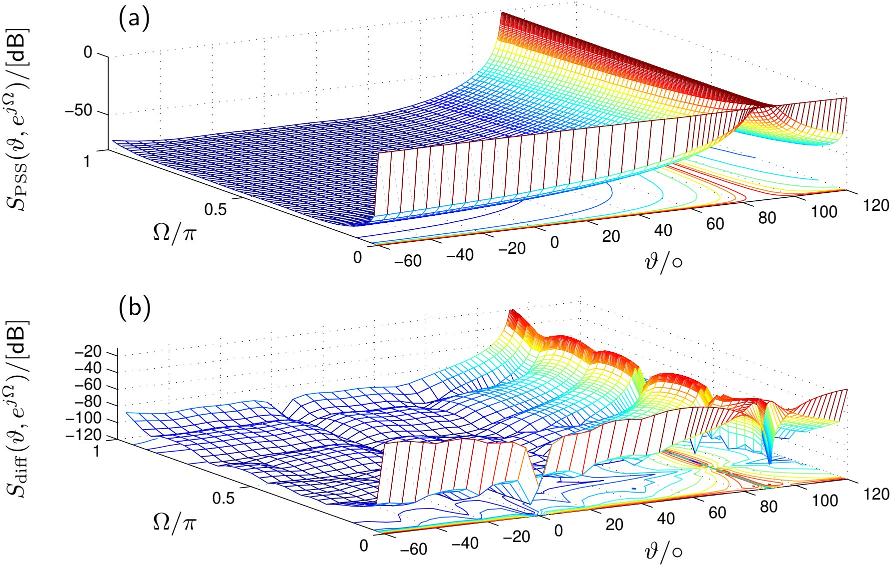

# Simulation II

- $M = 8$ element sensor array illuminated by three sources;
- source 1: $\vartheta_1 = -30°$, active over range $\Omega \in [\frac{3\pi}{8};\ \pi]$;
- source 2: $\vartheta_2 = 20°$, active over range $\Omega \in [\frac{\pi}{2};\ \pi]$;
- source 3: $\vartheta_3 = 40°$, active over range $\Omega \in [\frac{2\pi}{8};\ \frac{7\pi}{8}]$; and

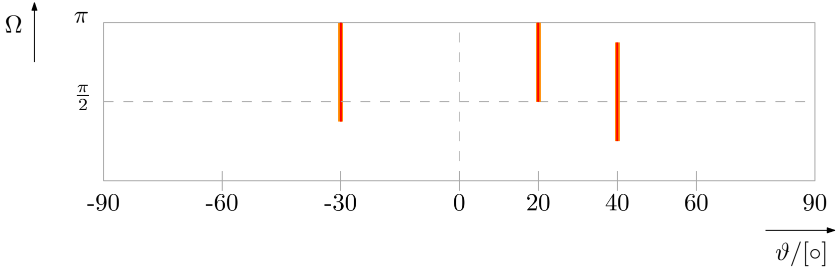


- filter banks as innovation filters, and broadband steering vectors to simulate AoA;
- space-time covariance matrix is estimated from $10^4$ samples.

# Simulation II — PSS-MUSIC

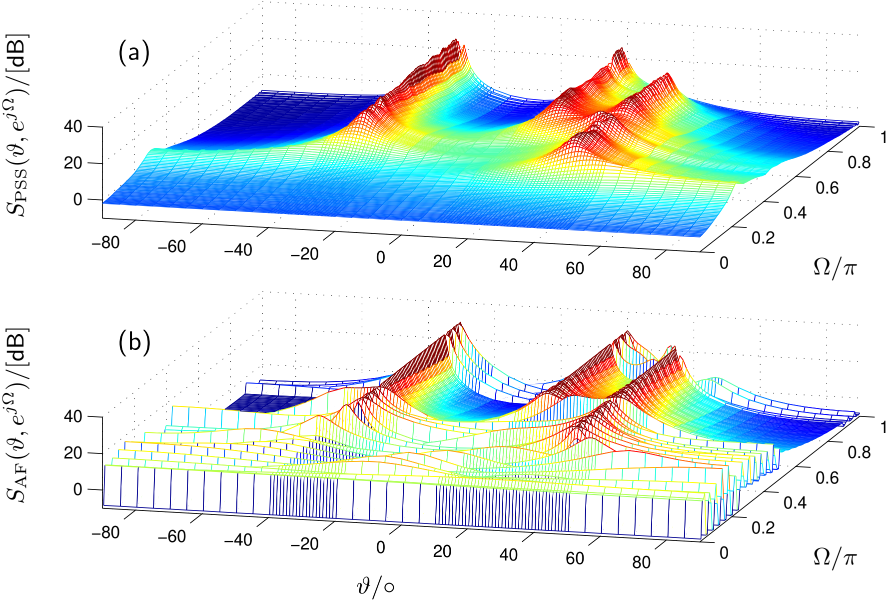

# PS-MUSIC Comparison

- Simulation I (toy problem): peaks normalised to unity:

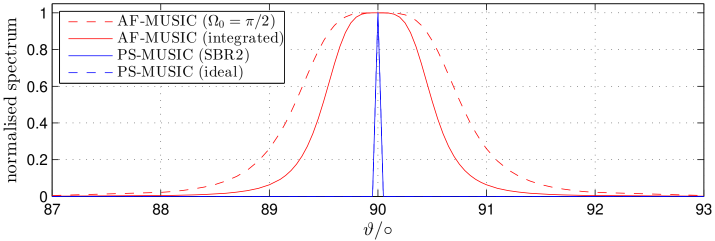


- Simulation II: inaccuracies on PEVD and broadband steering vector

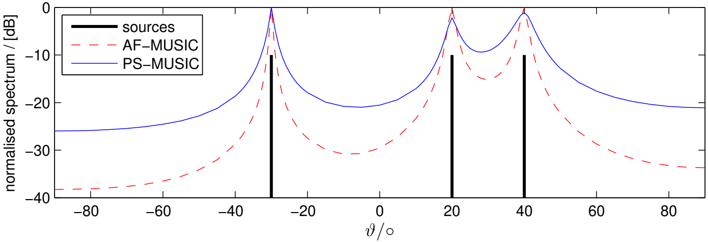

# AoA Estimation — Conclusions

- We have considered the importance of SVD and EVD for narrowband source separation;
- narrowband matrix decomposition real the matrix rank and offer subspace decompositions on which angle-of-arrival estimation alhorithms such as MUSIC can be based;
- broadband problems lead to a space-time covariance or CSD matrix;
- such polynomial matrices cannot be decomposed by standard EVD and SVD;
- a polynomial EVD has been defined;
- iterative algorithms such as SBR2 can be used to approximate the PEVD;
- this permits a number of applications, such as broadband angle of arrival estimation;
- broadband beamforming could then be used to separate broadband sources.

# Further Reading

- Multiple signal classification (MUSIC) algorithm [83] and polynomial MUSIC [12, 9];
- comparisons to other broadband AoA approaches:[10, 14, 98];
- construction of accurate steering vectors using fractional delay filters [51, 84]: [11, 13];
- polynomial MUSIC applied in an echoic speech scenario [48], and compared to an independent frequency-bin approach [106];
- impact of source model conditioning [24], algorithmic issues [33], and estimation errors [38, 41].

# Narrowband Minimum Variance Distortionless Response Beamformer

- Scenario: an array of $M$ sensors receives data $\mathbf{x}[n]$, containing a desired signal with frequency $\Omega_\mathrm{s}$ and angle of arrival $\vartheta_\mathrm{s}$, corrupted by interferers;
- a narrowband beamformer applies a single coefficient to every of the $M$ sensor signals:

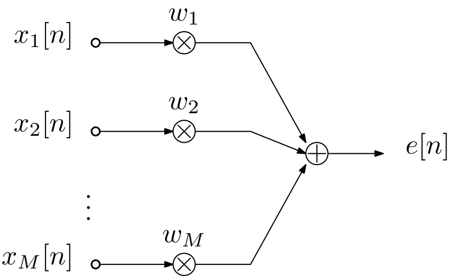

# Narrowband MVDR Problem

- Recall the space-time covariance matrix:

$$\mathbf{R}[\tau] = \mathcal{E}\{\mathbf{x}[n]\mathbf{x}^{\mathrm{H}}[n-\tau]\}$$

- the MVDR beamformer minimises the output power of the beamformer:

$$\min_{\mathbf{w}} \mathcal{E}\{|e[n]|^2\} = \min_{\mathbf{w}} \mathbf{w}^{\mathrm{H}}\mathbf{R}[0]\mathbf{w} \quad (40)$$

$$\text{s.t.} \quad \mathbf{a}^{\mathrm{H}}(\vartheta_{\mathrm{s}}, \Omega_{\mathrm{s}})\mathbf{w} = 1 \,, \quad (41)$$

- this is subject to protecting the signal of interest by a constraint in look direction $\vartheta_{\mathrm{s}}$;
- the steering vector $\mathbf{a}_{\vartheta_{\mathrm{s}},\Omega_{\mathrm{s}}}$ defines the signal of interest's parameters.

# Broadband MVDR Beamformer

- Each sensor is followed by a tap delay line of dimension $L$, giving a total of $ML$ coefficients in a vector $\mathbf{v} \in \mathbb{C}^{ML}$

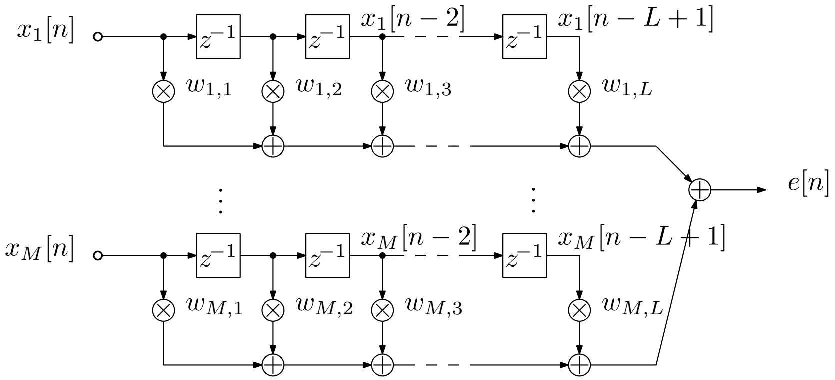

# Broadband MVDR Beamformer

- A larger input vector $\mathbf{x}_n \in \mathbb{C}^{ML}$ is generated, also including lags;
- the general approach is similar to the narrowband system, minimising the power of $e[n] = \mathbf{v}^{\mathrm{H}}\mathbf{x}_n$;
- however, we require several constraint equations to protect the signal of interest, e.g.

$$\mathbf{C} = [\mathbf{s}(\vartheta_{\mathrm{s}}, \Omega_0), \;\; \mathbf{s}(\vartheta_{\mathrm{s}}, \Omega_1) \; \ldots \; \mathbf{s}(\vartheta_{\mathrm{s}}, \Omega_{L-1})] \qquad (42)$$

- these $L$ constraints pin down the response to unit gain at $L$ separate points in frequency:

$$\mathbf{C}^{\mathrm{H}}\mathbf{v} = \mathbf{1} \; ; \qquad (43)$$

- generally $\mathbf{C} \in \mathbb{C}^{ML \times L}$, but simplifications can be applied if the look direction is towards broadside.

# Generalised Sidelobe Canceller

- A quiescent beamformer $\mathbf{v}_\mathrm{q} = \left(\mathbf{C}^\mathrm{H}\right)^\dagger \mathbf{1} \in \mathbb{C}^{ML}$ picks the signal of interest;
- the quiescent beamformer is optimal for AWGN but generally passes structured interference;
- the output of the blocking matrix $\mathbf{B}$ contains interference only, which requires $[\mathbf{BC}]$ to be unitary; hence $\mathbf{B} \in \mathbb{C}^{ML \times (M-1)L}$;
- an adaptive noise canceller $\mathbf{v}_\mathrm{a} \in \mathbb{C}^{(M-1)L}$ aims to remove the residual interference:

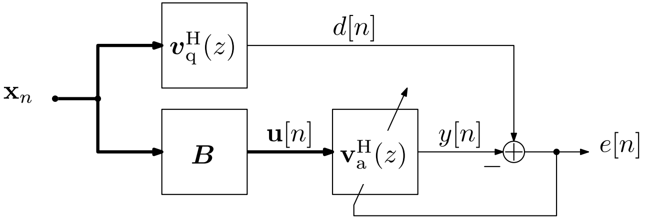


- note: all dimensions are determined by $\{M, L\}$.

# Polynomial Matrix MVDR Formulation

- Power spectral density of beamformer output: $R_e(z) = \tilde{\boldsymbol{w}}(z)\boldsymbol{R}(z)\boldsymbol{w}(z)$
- proposed broadband MVDR beamformer formulation:

$$\min_{\mathbf{w}(z)} \oint_{|z|=1} R_e(z)\frac{dz}{z} \quad (44)$$

$$\text{s.t.} \quad \tilde{\boldsymbol{a}}(\vartheta_{\rm s}, z)\boldsymbol{w}(z) = F(z) \; . \quad (45)$$

- precision of broadband steering vector, $|\tilde{\boldsymbol{a}}(\vartheta_{\rm s}, z)\boldsymbol{a}(\vartheta_{\rm s}, z) - 1|$, depends on the length $T$ of the fractional delay filter:

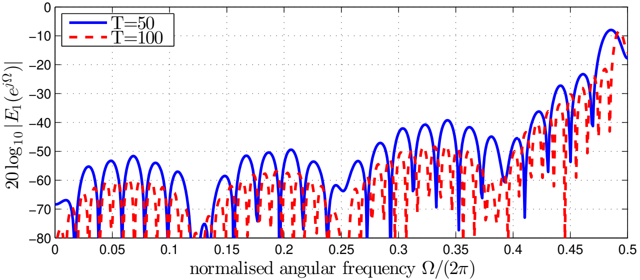

# Generalised Sidelobe Canceller

University of Strathclyde Engineering

- Instead of performing constrained optimisation, the GSC projects the data and performs adaptive noise cancellation:

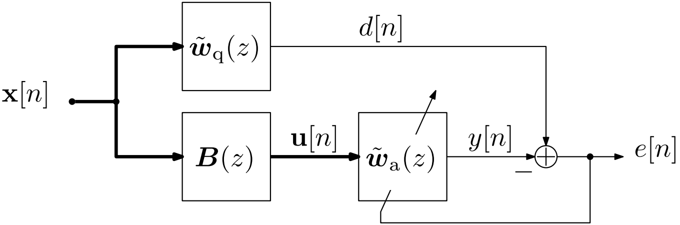


- the quiescent vector $\mathbf{w}_{\mathrm{q}}(z)$ is generated from the constraints and passes signal plus interference;
- the blocking matrix $\boldsymbol{B}(z)$ has to be orthonormal to $\mathbf{w}_{\mathrm{q}}(z)$ and only pass interference.

# Design Considerations

- The blocking matrix can be obtained by completing a paraunitary matrix from $\mathbf{w}_{\mathrm{q}}(z)$;
- this can be achieved by calculating a PEVD of the rank one matrix $\mathbf{w}_{\mathrm{q}}(z)\tilde{\mathbf{w}}_{\mathrm{q}}(z)$;
- this leads to a block matrix of order $N$ that is typically greater than $L$;
- maximum leakage of the signal of interest through the blocking matrix:

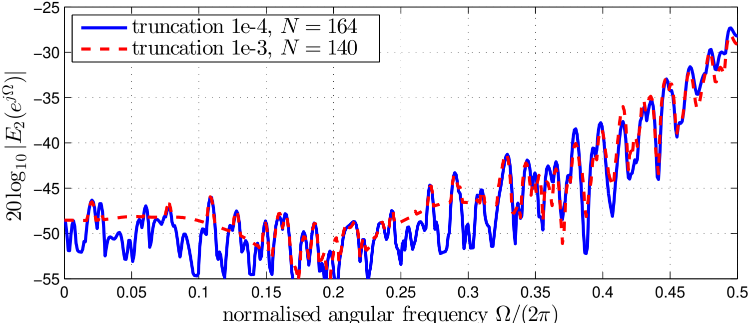

# Computational Cost

- With $M$ sensors and a TDL length of $L$, the complexity of a standard beamformer is dominated by the blocking matrix;
- in the proposed design, $\mathbf{w}_{\mathrm{a}} \in \mathbb{C}^{M-1}$ has degree $L$;
- the quiescent vector $\mathbf{w}_{\mathrm{q}}(z) \in \mathbb{C}^{M}$ has degree $T$;
- the blocking matrix $\boldsymbol{B}(z) \in \mathbb{C}^{(M-1)\times M}$ has degree $N$;
- cost comparison in multiply-accumulates (MACs):

| | GSC cost | |
|---|---|---|
| component | polynomial | standard |
| quiescent beamformer | $MT$ | $ML$ |
| blocking matrix | $M(M-1)N$ | $M(M-1)L^2$ |
| adaptive filter (NLMS) | $2(M-1)L$ | $2(M-1)L$ |

# Example

- We assume a signal of interest from $\vartheta = 30°$;
- three interferers with angles $\vartheta_i \in \{-40°, -10°, 80°\}$ active over the frequency range $\Omega = 2\pi \cdot [0.1;\ 0.45]$ at signal to interference ratio of -40 dB;

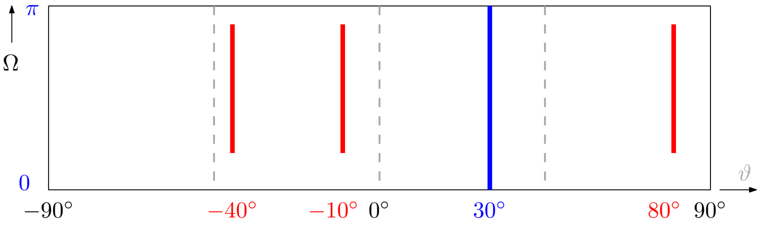


- $M = 8$ element linear uniform array is also corrupted by spatially and temporally white additive Gaussian noise at 20 dB SNR;
- parameters: $L = 175$, $T = 50$, and $N = 140$;
- cost per iteration: 10.7 kMACs (proposed) versus 1.72 MMACs (standard).

# Quiescent Beamformer

- Directivity pattern of quiescent standard broadband beamformer:

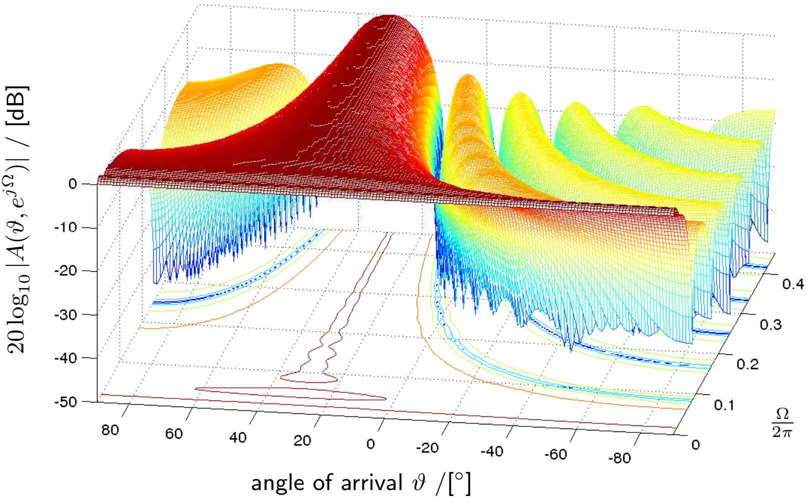

# Quiescent Beamformer

- Directivity pattern of quiescent proposed broadband beamformer:

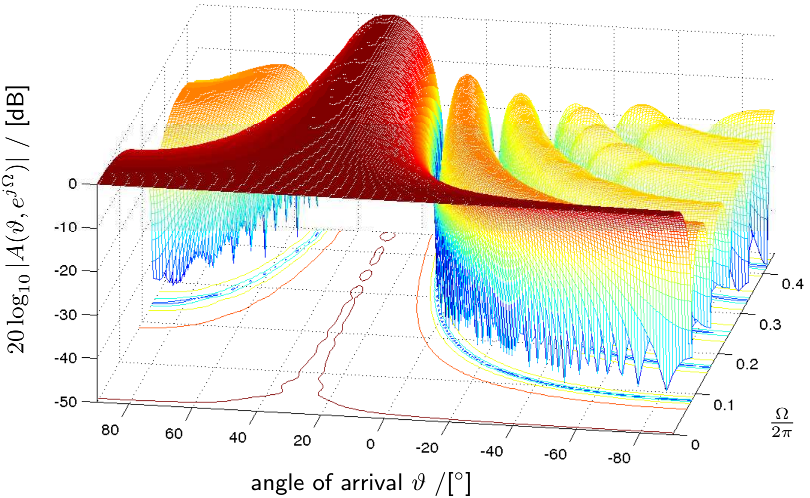

# Adaptation

- Convergence curves of the two broadband beamformers, showing the residual mean squared error (i.e. beamformer output minus signal of interest):

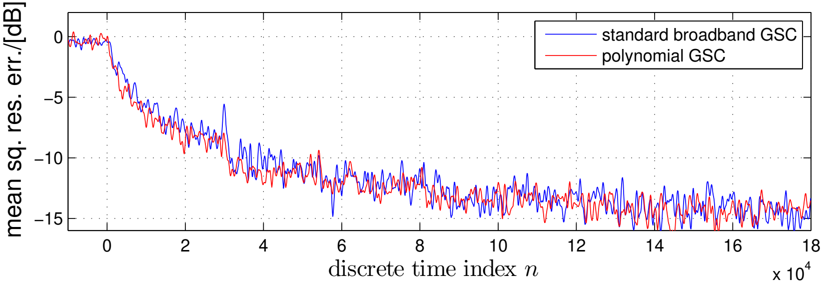

# Adapted Beamformer

- Directivity pattern of adapted proposed broadband beamformer:

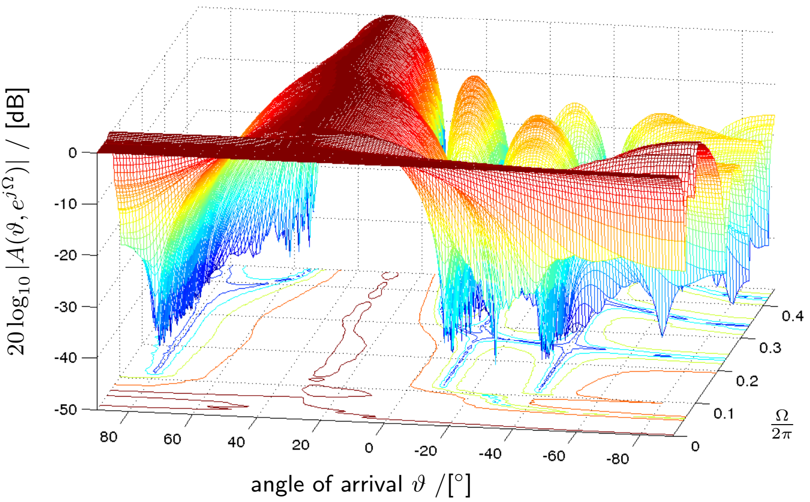

University of Strathclyde Engineering

# Adapted Beamformer

- Directivity pattern of adapted standard broadband beamformer:

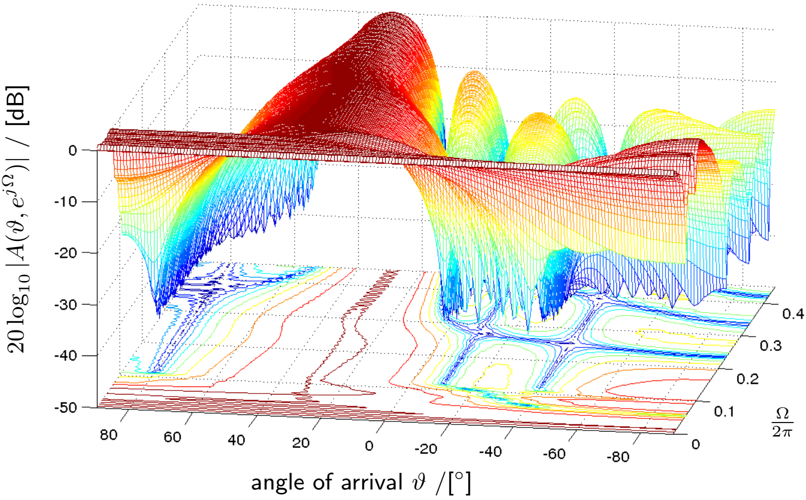

# Gain in Look Direction

- Gain in look direction $\vartheta_s = 30^\circ$ before and after adaptation:

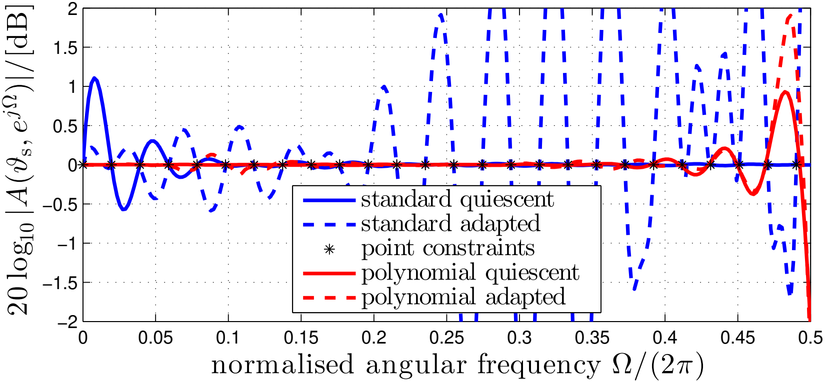


- due to signal leakage, the standard broadband beamformer after adaptation only maintains the point constraints but deviates elsewhere.

# Broadband Beamforming Conclusions

- Based on the previous AoA estimation, beamforming can help to extract source signals and thus perform "source separation";
- broadband beamformers usually assume pre-steering such that the signal of interest lies at broadside;
- this is not always given, and difficult for arbitary array geometries;
- the proposed beamformer using a polynomial matrix formulation can implement abitrary constraints;
- the performance for such constraints is better in terms of the accuracy of the directivity pattern;
- because the proposed design decouples the complexities of the coefficient vector, the quiescent vector and block matrix, and the adaptive process, the cost is significantly lower than for a standard broadband adaptive beamformer.

# Further Reading

- Basic idea of a polynomial MVDR/GSC beamformer: [99];
- investigation of constrained optimisation in the polynomial domain: [15];
- polynomial GSC for arbitrary 3d arrays: [16];
- polynomial matrix-based source separation is not discussed here but directly related: [80, 78];
- broadband subspace-based techniques: [100].

# Source-Sensor Transfer Functions

- We take $M$-array measurements of a single source:

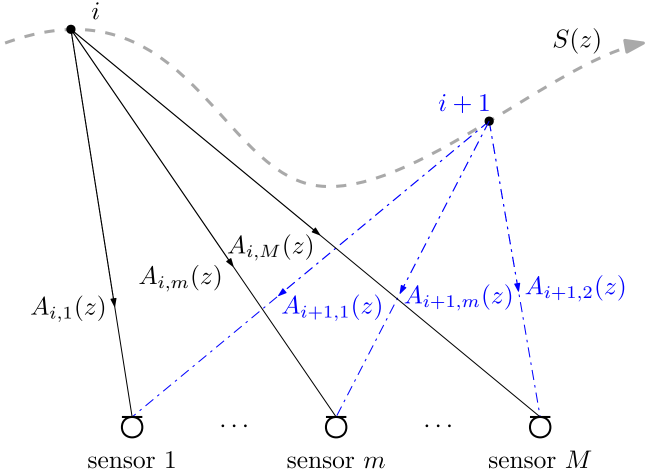


- 2nd order stats: $\boldsymbol{R}_i(z) = S(z)\boldsymbol{a}_i(z)\boldsymbol{a}_i^{\mathrm{P}}(z) = \gamma_i(z)\boldsymbol{u}_i(z)\boldsymbol{u}_i^{\mathrm{P}}$.

# Transfer Functions and PEVD

- 2nd order stats: $\boldsymbol{R}_i(z) = S(z)\boldsymbol{a}_i(z)\boldsymbol{a}_i^{\mathrm{P}}(z) = \gamma_{i,m}(z)\boldsymbol{u}_i(z)\boldsymbol{u}_i^{\mathrm{P}}$;
- difference: $\boldsymbol{u}_i(z)$ is normal, $\boldsymbol{u}_i^{\mathrm{P}}(z)\boldsymbol{u}_i(z) = 1$, while $\boldsymbol{a}_i(z)$ is not:

$$\boldsymbol{a}_i^{\mathrm{P}}(z)\boldsymbol{a}_i(z) = A_{i,(-)}(z)A_{i,(+)}(z) = A_{i,(+)}^{\mathrm{P}}(z)A_{i,(+)}(z)$$

  with minimum-phase $A_{(+)}(z)$;
- therefore:

$$H_i(z)\boldsymbol{u}_i(z) = \frac{\boldsymbol{a}_i(z)}{A_{i,(+)}(z)}$$

$$\gamma_i(z) = A_{i,(+)}(z)S(z)A_{i,(+)}^{\mathrm{P}}(z) \ ,$$

- from a single measurement $\boldsymbol{R}_i(z)$, we cannot say anything about $\boldsymbol{a}_i(z)$ or $S(z)$.

# Multiple Measurements

- If we have several measurements $i = 1 \ldots I$:

$$H_i(z)\boldsymbol{u}_i(z) = \frac{\boldsymbol{a}_i(z)}{A_{i,(+)}(z)}$$

$$\gamma_i(z) = A_{i,(+)}(z)S(z)A^{\mathrm{P}}_{i,(+)}(z) \; ,$$

- we can extract $S(z)$ as the greatest common divisor

$$\hat{S}(z) = \mathrm{GCD}\{\gamma_1(z) \; \ldots \; \gamma_I(z)\} \; ;$$

- we can then extract the terms $A_{i,(+)}(z)$, and hence determine the vectors $\boldsymbol{a}_i(z)$ save of an arbitrary phase response due to the allpass $H_i(z)$:

$$\boldsymbol{a}_i(z) = A_{i,(+)}(z)H_i(z)\boldsymbol{u}_i(z) \; .$$

# Alternative DFT Domain Attempt

- As an alternative, we take measurements in independent frequency bins $\Omega_k = \frac{2\pi k}{K}$:

$$\begin{aligned}\mathbf{R}_{i,k} = \boldsymbol{R}_i(e^{j\Omega_k}) &= \boldsymbol{a}_i(e^{j\Omega_k})S(e^{j\Omega_k})\boldsymbol{a}_i^{\mathrm{H}}(e^{j\Omega_k}) \\ &= \mathbf{q}_{i,k}\lambda_{i,k}\mathbf{q}_{i,k}^{\mathrm{H}} \ .\end{aligned}$$

- principal eigenvectors and eigenvalues for the measurement campaigns are

$$\begin{aligned}\mathbf{q}_{i,k} &= \frac{\boldsymbol{a}_i(e^{j\Omega_k})}{|\boldsymbol{a}_i(e^{j\Omega_k})|} \ , \\ \lambda_{i,k} &= S(e^{j\Omega_k})|\boldsymbol{a}_i(e^{j\Omega_k})|^2 \ .\end{aligned}$$

- because of the normalisation, nothing can be extracted about the source or the transfer functions.

# Numerical Example

- Source with power spectral density

$$S(z) = \frac{1}{2}z + \frac{5}{4} + \frac{1}{2}z^{-1}$$

- vector of transfer functions during campaign $i = 1$:

$$\boldsymbol{a}_1(z) = \begin{bmatrix} 1 & + & \frac{1}{2}z^{-1} \\ \frac{3}{4} & - & \frac{1}{2}z^{-1} \end{bmatrix}$$

- vector of transfer functions during campaign $i = 2$:

$$\boldsymbol{a}_2(z) = \begin{bmatrix} \frac{4}{5} & - & \frac{1}{2}z^{-1} \\ -\frac{1}{2} & + & z^{-1} \end{bmatrix} ;$$

- based on these: PEVD computations for $\boldsymbol{R}_1(z)$ and $\boldsymbol{R}_2(z)$, and GCD calculation based on eigenvalues.

# Numerical Results — Source PSD

- Eigenvalues / source PSD for both measurements $i = \{1, 2\}$:

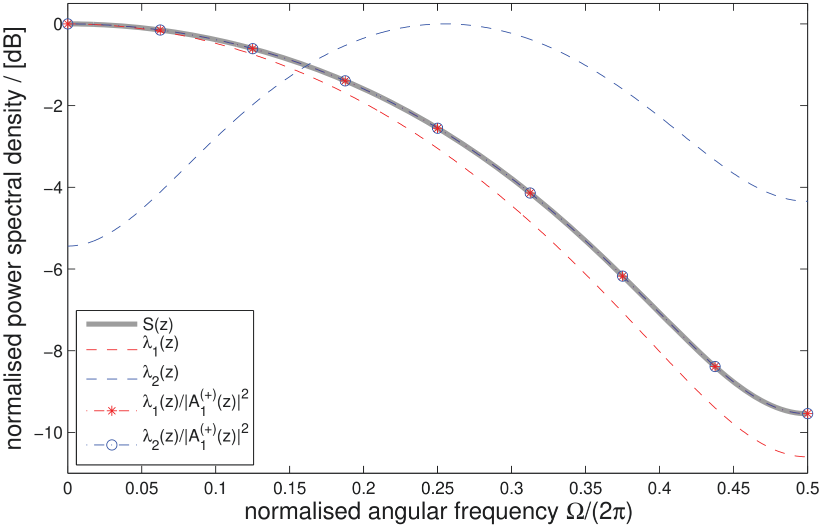

# Numerical Result — Magnitude Responses I

- Eigenvectors / magnitude response for measurement $i = \{1\}$:

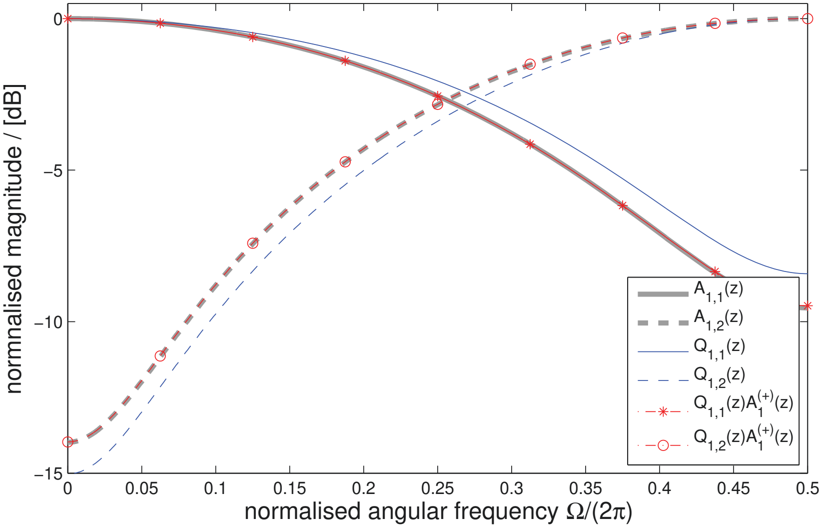

# Numerical Result — Magnitude Responses II

- Eigenvectors / magnitude response for measurement $i = \{2\}$:

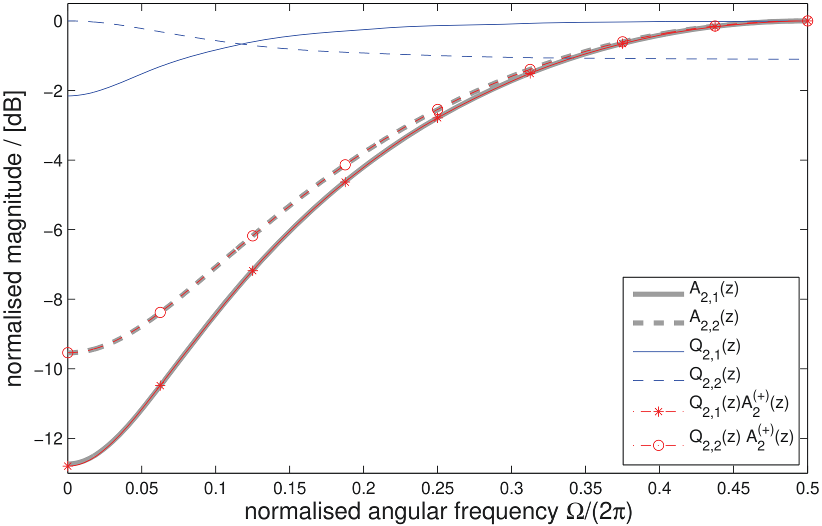

# Application Summary and Critique

- We can extract the source PSD and the magnitude responses once we have at least two measurements [101];
- an independent frequency bin approach does not yield anything;
- the polynomial approach rests on an accurate parahermitian EVD, and an accurate root finding / GCD algorithm;
- root finding is numerically challenging: research since Euclid (300BC), with robust root-finding methods still on-going (Gröbner bases, algebraic geometry);
- nevertheless the approach gives a glimpse of the type of advantages that a coherent broadband approach can offer.

# Further Reading

- This approach is discussed in [101];
- an additional application not elaborated here is speech dereverberation [75, 72, 74, 73].

# Additional Material

- Key papers:
  1. J.G. McWhirter, P.D. Baxter, T. Cooper, S. Redif, and J. Foster: "An EVD Algorithm for Para-Hermitian Polynomial Matrices," IEEE Trans SP, **55**(5): 2158-2169, May 2007.
  2. S. Redif, J.G. McWhirter, and S. Weiss: "Design of FIR Paraunitary Filter Banks for Subband Coding Using a Polynomial Eigenvalue Decomposition," IEEE Trans SP, **59**(11): 5253-5264, Nov. 2011.
  3. S. Redif, S. Weiss, and J.G. McWhirter: "Sequential matrix diagonalisation algorithms for polynomial EVD of parahermitian matrices," IEEE Trans SP, **63**(1): 81–89, Jan. 2015.
- If interested in the discussed methods and algorithms, please download the free Matlab PEVD toolbox from

  pevd-toolbox.eee.strath.ac.uk
- for questions, please feel free to ask:
  - Stephan Weiss (stephan.weiss@strath.ac.uk) or
  - Connor Deloasa (connor.delaosa@strath.ac.uk)
  - Faizan Khattak (faizan.khattak@strath.ac.uk)

# References I

[1] W. Al-Hanafy, A. P. Millar, C. H. Ta, and S. Weiss.
Broadband SVD and non-linear precoding applied to broadband MIMO channels.
In *42nd Asilomar Conference on Signals, Systems and Computers*, pages 2053–2057, Pacific Grove, CA, USA, Oct. 2008.

[2] W. Al-Hanafy and S. Weiss.
Comparison of precoding methods for broadband mimo systems.
In *Third International Workshop on Computational Advances in Multi-Sensor Adaptive Processing*, Aruba, Dutch Antilles, Dec. 2009.

[3] W. Al-Hanafy and S. Weiss.
A new low-cost discrete bit loading using greedy power allocation.
In *Third Mosharaka International Conference on Communications, Computers and Applications*, Amman, Jordan, October 2009.
(best paper award).

[4] W. Al-Hanafy and S. Weiss.
Sum-rate maximisation comparison using incremental approaches with different constraints.
In *Third Mosharaka International Conference on Communications, Computers and Applications*, Amman, Jordan, October 2009.

[5] W. Al-Hanafy and S. Weiss.
Greedy power allocation for multicarrier systems with reduced complexity.
In *National Radio Science Conference*, Menoufia, Egypt, March 2010.

[6] W. Al-Hanafy and S. Weiss.
Reduced complexity schemes to greedy power allocation for multicarrier systems.
In *18th International Conference on Microwave, Radar and Wireless Communications*, 2010.

[7] W. Al-Hanafy and S. Weiss.
Trade-off between complexity and ber performance of a polynomial svd-based broadband mimo transceiver.
In *27th National Radio Science Conference*, Menoufia, Egypt, March 2010.

# References II

[8] W. Al-Hanafy and S. Weiss.
An adaptive modulation precoding scheme for mean ber minimisation of isi mimo channels.
In *19th European Signal Processing Conference*, pages 1638–1642, Barcelona, Spain, August 2011.

[9] M. Alrmah, J. Corr, A. Alzin, K. Thompson, and S. Weiss.
Polynomial subspace decomposition for broadband angle of arrival estimation.
In *Sensor Signal Processing for Defence*, pages 1–5, Edinburgh, Scotland, Sept 2014.

[10] M. Alrmah, M. Hussin, S. Weiss, and S. Lambotharan.
Comparison of broadband direction of arrival estimation algorithms.
In *9th IMA Mathematics in Signal Processing Conference*, Birmingham, UK, December 2012.

[11] M. Alrmah and S. Weiss.
Filter bank based fractional delay filter implementation for widely accurate broadband steering vectors.
In *5th IEEE International Workshop on Computational Advances in Multi-Sensor Adaptive Processing*, Saint Martin, December 2013.

[12] M. Alrmah, S. Weiss, and S. Lambotharan.
An extension of the MUSIC algorithm to broadband scenarios using polynomial eigenvalue decomposition.
In *19th European Signal Processing Conference*, pages 629–633, Barcelona, Spain, August 2011.

[13] M. Alrmah, S. Weiss, and J. McWhirter.
Implementation of accurate broadband steering vectors for broadband angle of arrival estimation.
In *IET Intelligent Signal Processing*, London, UK, December 2013.

[14] M. Alrmah, S. Weiss, S. Redif, S. Lambotharan, and J. McWhirter.
Angle of arrival estimation for broadband signals: A comparison.
In *IET Intelligent Signal Processing*, London, UK, December 2013.

[15] A. Alzin, F. Coutts, J. Corr, S. Weiss, I. Proudler, and J. Chambers.
Polynomial matrix formulation-based Capon beamformer.
In *IMA International Conference on Signal Processing in Mathematics*, Birmingham, UK, December 2016.

# References III

[16] A. Alzin, F. Coutts, J. Corr, S. Weiss, I. K. Proudler, and J. A. Chambers.
Adaptive broadband beamforming with arbitrary array geometry.
In *IET/EURASIP Intelligent Signal Processing*, London, UK, December 2015.

[17] V. Anis, C. Delaosa, L. H. Crockett, and S. Weiss.
Energy-efficient wideband transceiver with per-band equalisation and synchronisation.
In *IEEE Wireless Communications and Networking Conference*, April 2018.

[18] J. Corr, J. Pestana, S. Redif, I. Proudler, and Moonen.
Investigation of a polynomial matrix generalised evd for multi-channel wiener filtering.
In *50th Asilomar Conference on Signals Systems and Computers*, Pacific Grove, CA, November 2016.

[19] J. Corr, K. Thompson, S. Weiss, J. McWhirter, and I. Proudler.
Cyclic-by-row approximation of iterative polynomial EVD algorithms.
In *Sensor Signal Processing for Defence*, pages 1–5, Edinburgh, Scotland, Sept 2014.

[20] J. Corr, K. Thompson, S. Weiss, J. McWhirter, and I. Proudler.
Maximum energy sequential matrix diagonalisation for parahermitian matrices.
In *48th Asilomar Conference on Signals, Systems and Computers*, pages 470–474, Pacific Grove, CA, USA, November 2014.

[21] J. Corr, K. Thompson, S. Weiss, J. McWhirter, and I. Proudler.
Performance trade-offs in sequential matrix diagonalisation search strategies.
In *IEEE 6th International Workshop on Computational Advances in Multi-Sensor Adaptive Processing*, pages 25–28, Cancun, Mexico, December 2015.

[22] J. Corr, K. Thompson, S. Weiss, J. McWhirter, S. Redif, and I. Proudler.
Multiple shift maximum element sequential matrix diagonalisation for parahermitian matrices.
In *IEEE Workshop on Statistical Signal Processing*, pages 312–315, Gold Coast, Australia, June 2014.

# References IV

University of Strathclyde Engineering


[23] J. Corr, K. Thompson, S. Weiss, J. G. McWhirter, and I. K. Proudler.
Causality-Constrained multiple shift sequential matrix diagonalisation for parahermitian matrices.
In *22nd European Signal Processing Conference*, pages 1277–1281, Lisbon, Portugal, September 2014.

[24] J. Corr, K. Thompson, S. Weiss, I. Proudler, and J. McWhirter.
Impact of source model matrix conditioning on PEVD algorithms.
In *IET/EURASIP Intelligent Signal Processing*, London, UK, December 2015.

[25] J. Corr, K. Thompson, S. Weiss, I. Proudler, and J. McWhirter.
Reduced search space multiple shift maximum element sequential matrix diagonalisation algorithm.
In *IET/EURASIP Intelligent Signal Processing*, London, UK, December 2015.

[26] J. Corr, K. Thompson, S. Weiss, I. Proudler, and J. McWhirter.
Row-shift corrected truncation of paraunitary matrices for PEVD algorithms.
In *23rd European Signal Processing Conference*, pages 849–853, Nice, France, August/September 2015.

[27] J. Corr, K. Thompson, S. Weiss, I. Proudler, and J. McWhirter.
Shortening of paraunitary matrices obtained by polynomial eigenvalue decomposition algorithms.
In *Sensor Signal Processing for Defence*, Edinburgh, Scotland, September 2015.

[28] F. Coutts, J. Corr, K. Thompson, I. Proudler, and S. Weiss.
Divide-and-conquer sequential matrix diagonalisation for parahermitian matrices.
In *Sensor Signal Processing for Defence Conference*, pages 1–5, London, UK, December 2017.

[29] F. Coutts, J. Corr, K. Thompson, S. Weiss, P. I.K., and J. McWhirter.
Multiple shift QR decomposition for polynomial matrices.
In *IMA International Conference on Mathematics in Signal Processing*, Birmingham, UK, December 2016.

[30] F. Coutts, J. Corr, K. Thompson, S. Weiss, I. Proudler, and J. McWhirter.
Complexity and search space reduction in cyclic-by-row PEVD algorithms.
In *50th Asilomar Conference on Signals, Systems and Computers*, Pacific Grove, CA, November 2016.

# References V


[31] F. Coutts, K. Thompson, I. Proudler, and S. Weiss.
Restricted update sequential matrix diagonalisation for parahermitian matrices.
In *IEEE 7th International Workshop on Computational Advances in Multi-Sensor Adaptive Processing*, Curacao, December 2017.

[32] F. Coutts, K. Thompson, S. Weiss, and I. Proudler.
A comparison of iterative and DFT-based polynomial matrix eigenvalue decompositions.
In *IEEE 7th International Workshop on Computational Advances in Multi-Sensor Adaptive Processing*, Curacao, December 2017.

[33] F. Coutts, K. Thompson, S. Weiss, and I. Proudler.
Impact of fast-converging PEVD algorithms on broadband AoA estimation.
In *Sensor Signal Processing for Defence Conference*, pages 1–5, London, UK, December 2017.

[34] F. K. Coutts, J. Corr, K. Thompson, S. Weiss, I. Proudler, and J. G. McWhirter.
Memory and complexity reduction in parahermitian matrix manipulations of PEVD algorithms.
In *24th European Signal Processing Conference*, Budapest, Hungary, Aug. 2016.

[35] F. K. Coutts, I. K. Proudler, and S. Weiss.
Efficient implementation of iterative polynomial matrix evd algorithms exploiting structural redundancy and parallelisation.
*IEEE Transactions on Circuits and Systems I: Regular Papers*, 66(12):4753–4766, Dec. 2019.

[36] F. K. Coutts, K. Thompson, J. Pestana, I. Proudler, and S. Weiss.
Enforcing eigenvector smoothness for a compact DFT-based polynomial eigenvalue decomposition.
In *10th IEEE Workshop on Sensor Array and Multichannel Signal Processing*, pages 1–5, July 2018.

[37] F. K. Coutts, K. Thompson, S. Weiss, and I. K. Proudler.
Analysing the performance of divide-and-conquer sequential matrix diagonalisation for large broadband sensor arrays.
In *2017 IEEE International Workshop on Signal Processing Systems*, pages 1–6, Lorient, France, October 2017.

# References VI

University of Strathclyde Engineering

[38] C. Delaosa, F. K. Coutts, J. Pestana, and S. Weiss.
Impact of space-time covariance estimation errors on a parahermitian matrix EVD.
In *10th IEEE Workshop on Sensor Array and Multichannel Signal Processing*, pages 1–5, July 2018.

[39] C. Delaosa, J. Pestana, N. J. Goddard, S. Somasundaram, and S. Weiss.
Sample space-time covariance matrix estimation.
In *ICASSP 2019 - 2019 IEEE International Conference on Acoustics, Speech and Signal Processing (ICASSP)*, pages 8033–8037, May 2019.

[40] C. Delaosa, J. Pestana, N. J. Goddard, S. D. Somasundaram, and S. Weiss.
Support estimation of a sample space-time covariance matrix.
In *Sensor Signal Processing for Defence*, Brighton, UK, March 2019.

[41] C. Delaosa, J. Pestana, S. Weiss, and P. I.K.
Subspace perturbation bounds with an application to angle ofarrival estimation using the music algorithm.
In *International Conference on Sensor Signal Processing for Defence*, 2020.

[42] N. J. Fliege.
*Multirate Digital Signal Processing: Multirate Systems, Filter Banks, Wavelets.*
John Wiley & Sons, Chichester, 1994.

[43] J. Foster, J. McWhirter, M. Davies, and J. Chambers.
An algorithm for calculating the qr and singular value decompositions of polynomial matrices.
*IEEE Transactions on Signal Processing*, 58(3):1263–1274, March 2010.

[44] J. Foster, J. McWhirter, S. Lambotharan, I. Proudler, M. Davies, and J. Chambers.
Polynomial matrix qr decomposition for the decoding of frequency selective multiple-input multiple-output communication channels.
*IET Signal Processing*, 6(7):704–712, September 2012.

# References VII

[45] I. Gohberg, P. Lancaster, and L. Rodman.
*Matrix Polynomials*.
Academic Press, New York, 1982.

[46] G. H. Golub and C. F. Van Loan.
*Matrix Computations*.
John Hopkins University Press, Baltimore, Maryland, 3rd edition, 1996.

[47] D. Hassan, S. Redif, J. G. McWhirter, and S. Lambotharan.
Polynomial gsvd beamforming for two-user frequency-selective mimo channels.
*IEEE Transactions on Signal Processing*, 69:948–959, 2021.

[48] A. Hogg, V. Neo, S. Weiss, C. Evers, and P. Naylor.
A polynomial eigenvalue decomposition music approach for broadband sound source localization.
In *Proc. IEEE Workshop on Applications of Signal Processing to Audio and Acoustics*, New Paltz, NY, Oct. 2021.

[49] S. Kasap and S. Redif.
Novel field-programmable gate array architecture for computing the eigenvalue decomposition of para-hermitian polynomial matrices.
*IEEE Transactions on Very Large Scale Integration (VLSI) Systems*, 22(3):522–536, March 2014.

[50] F. A. Khattak, S. Weiss, and I. K. Proudler.
Fast givens rotation approach to second order sequential best rotation algorithms.
In *International Conference in Sensor Signal Processing for Defence*, pages 40–44, Edinburgh, Scotland, September 2021.

[51] T. I. Laakso, V. Välimäki, M. Karjalainen, and U. K. Laine.
Splitting the Unit Delay.
*IEEE Signal Processing Magazine*, 13(1):30–60, January 1996.

# References VIII


[52] P. Lancaster and M. Tismenetsky.
*The Theory of Matrices*.
Academic Press, 1985.

[53] C. Liu, M. Hadef, C. H. Ta, and S. Weiss.
A Coding and Equalisation Approach for Dispersive Channels with Structured Additive Noise.
In S. Weiss, editor, *IEE/EURASIP Conference on DSP Enabled Radio*, volume 2005/11086, pages 33/1–33/4, Southampton, UK, September 2005.

[54] C. Liu, C. H. Ta, and S. Weiss.
Joint precoding and equalisation design using oversampled filter banks for dispersive channels with correlated noise.
In *IEEE Workshop on Signal Processing Systems*, pages 232–236, Shanghai, China, October 2007.

[55] C. Liu. and S. Weiss.
A precoding and equalisation design based on oversampled filter banks for dispersive channels with correlated noise.
In *15th European Signal Processing Conference*, pages 511–514, Poznan, Poland, September 2007.

[56] C. Liu, S. Weiss, S. Redif, T. Cooper, L. Lampe, and J. G. McWhirter.
Channel Coding for Power Line Communication Based on Oversampled Filter Banks.
In L. Lampe, editor, *International Symposium on Power Line Communications and Its Applications*, pages 246–249, Vancouver, CA, April 6-8 2005.

[57] J. G. McWhirter and P. D. Baxter.
A Novel Technqiue for Broadband SVD.
In *12th Annual Workshop on Adaptive Sensor Array Processing*, MIT Lincoln Labs, Cambridge, MA, 2004.

[58] J. G. McWhirter, P. D. Baxter, T. Cooper, S. Redif, and J. Foster.
An EVD Algorithm for Para-Hermitian Polynomial Matrices.
*IEEE Transactions on Signal Processing*, 55(5):2158–2169, May 2007.

# References IX


[59] A. Millar, S. Weiss, and R. Stewart.
THP transceiver design for MIMO relaying with direct link and partial CSI.
*IEEE Communications Letters*, 17(6):1204–1207, May 2013.

[60] A. Millar, S. Weiss, and R. Stewart.
Training based channel estimation algorithms for dual hop MIMO OFDM relay systems.
*IEEE Transactions on Communications*, 63(12):4711–4726, December 2015.

[61] A. P. Millar and S. Weiss.
Design of ZF and MMSE filter-banks in relay networks with average and peak power constraints.
In *IEEE Workshoop on Statistical Signal Processing*, Cardiff, UK, August 2009.

[62] A. P. Millar and S. Weiss.
Transceiver design for non-regenerative MIMO relay systems with decision feedback detection.
In *18th European Signal Processing Conference*, pages 402–406, Aalborg, Denmark, August 2010.

[63] A. P. Millar, S. Weiss, and R. W. Stewart.
Precoder design for MIMO relay networks with direct link and decision feedback equalisation.
*IEEE Communications Letters*, 15(10):1044–1046, October 2011.

[64] A. P. Millar, S. Weiss, and R. W. Stewart.
Tomlinson Harashima precoding design for non-regenerative MIMO relay networks.
In *IEEE 73rd Vehicular Technology Conference*, pages 1–5, Budapest, Hungary, May 2011.

[65] A. P. Millar, S. Weiss, and R. W. Stewart.
Tomlinson-Harashima precoding design for non-regenerative multicarrier MIMO relays.
*Q2 Working Paper 1, to be considered for submission to IEEE Transactions on Signal Processing.*, November 2011.
(15 page manuscript, to be submitted pending Motorola Mobility agreement).

[66] A. P. Millar, S. Weiss, and R. W. Stewart.
ZF DFE transceiver design for MIMO relay systems with direct source-destination link.
In *19th European Signal Processing Conference*, pages 1824–1828, Barcelona, Spain, August 2011.

# References X

[67] A. P. Millar, S. Weiss, and R. W. Stewart.
Robust transceiver design for mimo relay systems with tomlinson harashima precoding.
In *20th European Signal Processing Conference*, pages 1374–1378, Bukarest, Romania, August 2012.

[68] N. Moret, A. Tonello, and S. Weiss.
Mimo precoding for filter bank modulation systems based on psvd.
In *IEEE 73rd Vehicular Technology Conference*, pages 1–5, May 2011.
(best paper award).

[69] A. Nagy and S. Weiss.
Comparison of different filter-bank based multicarrier systems with fractionally spaced equalisation.
In *IMA International Conference on Mathematics in Signal Processing*, Birmingham, UK, December 2016.

[70] A. Nagy and S. Weiss.
Synchronisation and equalisation of an fbmc/oqam system by a polynomial matrix pseudo-inverse.
In *IEEE International Symposium on Signal Processing and Information Technology*, Bilbao, December 2017.

[71] A. A. Nagy and S. Weiss.
Channel equalisation of a MIMO FBMC/OQAM system using a polynomial matrix pseudo-inverse.
In *10th IEEE Workshop on Sensor Array and Multichannel Signal Processing*, April 2018.

[72] V. W. Neo, C. Evers, and P. A. Naylor.
Pevd-based speech enhancement in reverberant environments.
In *ICASSP 2020 - 2020 IEEE International Conference on Acoustics, Speech and Signal Processing (ICASSP)*, pages 186–190, 2020.

[73] V. W. Neo, C. Evers, and P. A. Naylor.
Polynomial matrix eigenvalue decomposition of spherical harmonics for speech enhancement.
In *ICASSP 2021 - 2021 IEEE International Conference on Acoustics, Speech and Signal Processing (ICASSP)*, pages 786–790, 2021.

# References XI

[74] V. W. Neo, C. Evers, and P. A. Naylor.
Speech dereverberation performance of a polynomial-evd subspace approach.
In *2020 28th European Signal Processing Conference (EUSIPCO)*, pages 221–225, 2021.

[75] V. W. Neo and P. A. Naylor.
Second order sequential best rotation algorithm with householder reduction for polynomial matrix eigenvalue decomposition.
In *IEEE International Conference on Acoustics, Speech and Signal Processing*, pages 8043–8047, Brighton, UK, May 2019.

[76] S. Redif, J. McWhirter, and S. Weiss.
Design of FIR paraunitary filter banks for subband coding using a polynomial eigenvalue decomposition.
*IEEE Transactions on Signal Processing*, 59(11):5253–5264, November 2011.

[77] S. Redif, J. G. McWhirter, and S. Weiss.
Design of orthonormal subband coders using polynomial eigenvalue decomposition.
*IEEE Transactions on Signal Processing*, 2010.
(submitted).

[78] S. Redif, J. Pestana, and I. K. Proudler.
Analysis of broadband GEVD-based blind source separation.
In *ICASSP 2019 - 2019 IEEE International Conference on Acoustics, Speech and Signal Processing (ICASSP)*, pages 8028–8032, Brighton, UK, May 2019.

[79] S. Redif, S. Weiss, and J. McWhirter.
Sequential matrix diagonalization algorithms for polynomial EVD of parahermitian matrices.
*IEEE Transactions on Signal Processing*, 63(1):81–89, January 2015.

[80] S. Redif, S. Weiss, and J. McWhirter.
Relevance of polynomial matrix decompositions to broadband blind signal separation.
*Signal Processing*, 134:76–86, May 2017.

# References XII

University of Strathclyde Engineering

[81] S. Redif, S. Weiss, and J. G. McWhirter.
An approximate polynomial matrix eigenvalue decomposition algorithm for para-hermitian matrices.
In *11th IEEE International Symposium on Signal Processing and Information Technology*, pages 421–425, Bilbao, Spain, December 2011.

[82] F. Rellich.
Störungstheorie der Spektralzerlegung. I. Mitteilung. Analytische Störung der isolierten Punkteigenwerte eines beschränkten Operators.
*Mathematische Annalen*, 113:DC–DCXIX, 1937.

[83] R. O. Schmidt.
Multiple emitter location and signal parameter estimation.
*IEEE Transactions on Antennas and Propagation*, 34(3):276–280, March 1986.

[84] J. Selva.
An efficient structure for the design of variable fractional delay filters based on the windowing method.
*IEEE Transactions on Signal Processing*, 56(8):3770–3775, August 2008.

[85] C. H. Ta, C. Liu, and S. Weiss.
An approach for block transmission based precoding and equalisation with improved performance.
In *IEEE International Symposium on Power Line Communications and Its Applications*, pages 331–335, Jeju Island, Korea, April 2008.

[86] C. H. Ta and S. Weiss.
Design of Precoding and Equalisation for MIMO Broadband Transmission.
In S. Weiss, editor, *IEE/EURASIP Conference on DSP Enabled Radio*, volume 2005/11086, pages 30/1–30/5, Southampton, UK, September 2005.

[87] C. H. Ta and S. Weiss.
A Design of Precoding and Equalisation for Broadband MIMO Systems.
In *15th International Conference on Digital Signal Processing*, pages 571–574, Cardiff, UK, July 2007.

# References XIII


[88] C. H. Ta and S. Weiss.
A design of precoding and equalisation for broadband MIMO systems.
In *Forty-First Asilomar Conference on Signals, Systems and Computers*, pages 1616–1620, Pacific Grove, CA, USA, Nov. 2007.

[89] C. H. Ta and S. Weiss.
A Jointly Optimal Precoder and Block Decision Feedback Equaliser Design With Low Redundancy.
In *15th European Signal Processing Conference*, pages 489–492, Poznan, Poland, September 2007.

[90] C. H. Ta and S. Weiss.
Shortening the order of paraunitary matrices in SBR2 algorithm.
In *6th International Conference on Information, Communications & Signal Processing*, pages 1–5, Singapore, Dec. 2007.

[91] M. Tohidian, H. Amindavar, and A. M. Reza.
A DFT-based approximate eigenvalue and singular value decomposition of polynomial matrices.
*EURASIP Journal on Advances in Signal Processing*, 2013(1):1–16, 2013.

[92] P. P. Vaidyanathan.
Multirate Digital Filters, Filter Banks, Polyphase Networks, and Applications: A Tutorial.
*Proceedings of the IEEE*, 78(1):56–93, January 1990.

[93] P. P. Vaidyanathan.
*Multirate Systems and Filter Banks*.
Prentice Hall, Englewood Cliffs, 1993.

[94] Z. Wang, J. McWhirter, J. Corr, and S. Weiss.
Order-controlled multiple shift sbr2 algorithm for para-hermitian polynomial matrices.
In *9th IEEE Sensor Array and Multichannel Signal Processing Workshop*, Rio de Janeiro, Brazil, July 2016.

# References XIV


[95] Z. Wang, J. G. McWhirter, J. Corr, and S. Weiss.
Multiple shift second order sequential best rotation algorithm for polynomial matrix EVD.
In *23rd European Signal Processing Conference*, pages 844–848, Nice, France, September 2015.

[96] S. Weiss.
Design of Overcomplete Expansions for Channel Coding.
In *6th IMA International Conference on Mathematics in Signal Processing*, volume 1, pages 215–218, Royal Agricultural College, Cirencester, UK, December 14–16, 2004.

[97] S. Weiss.
On the design of oversampled filter banks for channel coding.
In *European Signal Processing Conference*, volume 1, pages 885–888, Vienna, Austria, September 2004. invited paper.

[98] S. Weiss, M. Alrmah, S. Lambotharan, J. McWhirter, and M. Kaveh.
Broadband angle of arrival estimation methods in a polynomial matrix decomposition framework.
In *IEEE 5th International Workshop on Computational Advances in Multi-Sensor Adaptive Processing*, pages 109–112, Dec 2013.

[99] S. Weiss, S. Bendoukha, A. Alzin, F. Coutts, I. Proudler, and J. Chambers.
MVDR broadband beamforming using polynomial matrix techniques.
In *23rd European Signal Processing Conference*, pages 839–843, Nice, France, September 2015.

[100] S. Weiss, C. Delaosa, J. Matthews, I. Proudler, and B. Jackson.
Detection of weak transient signals using a broadband subspace approach.
In *International Conference on Sensor Signal Processing for Defence*, pages 65–69, Edinburgh, Scotland, Sept. 2021.

[101] S. Weiss, N. J. Goddard, S. Somasundaram, I. K. Proudler, and P. A. Naylor.
Identification of broadband source-array responses from sensor second order statistics.
In *Sensor Signal Processing for Defence Conference*, pages 1–5, London, UK, December 2017.

# References XV


[102] S. Weiss and M. D. Macleod.
Maximally smooth dirichlet interpolation from complete and incomplete sample points on the unit circle.
In *IEEE International Conference on Acoustics, Speech, and Signal Processing*, Brighton, UK, May 2019.

[103] S. Weiss, J. Pestana, I. Proudler, and F. Coutts.
Corrections to on the existence and uniqueness of the eigenvalue decomposition of a parahermitian matrix.
*IEEE Transactions on Signal Processing*, 66(23):6325–6327, Dec 2018.

[104] S. Weiss, J. Pestana, and I. K. Proudler.
On the existence and uniqueness of the eigenvalue decomposition of a parahermitian matrix.
*IEEE Transactions on Signal Processing*, 66(10):2659–2672, May 2018.

[105] S. Weiss, I. Proudler, F. Coutts, and J. Deeks.
Extraction of analytic eigenvectors from a parahermitian matrix.
In *International Conference on Sensor Signal Processing or Defence*, E, 2020.

[106] S. Weiss and I. K. Proudler.
Comparing Efficient Broadband Beamforming Architectures and Their Performance Trade-Offs.
In *14th International Conference on Digital Signal Processing*, volume I, pages 417–422, Santorini, Greece, July 1–3 2002.
(invited paper).

[107] S. Weiss, I. K. Proudler, and F. K. Coutts.
Eigenvalue decomposition of a parahermitian matrix: Extraction of analytic eigenvalues.
*IEEE Transactions on Signal Processing*, 69:722–737, 2021.

[108] S. Weiss, I. K. Proudler, F. K. Coutts, and J. Pestana.
Iterative approximation of analytic eigenvalues of a parahermitian matrix EVD.
In *IEEE International Conference on Acoustics, Speech and Signal Processing*, Brighton, UK, May 2019.

# References XVI


[109] S. Weiss, I. K. Proudler, and M. D. Macleod.
Measuring smoothness of real-valued functions defined by sample points on the unit circle.
In *Sensor Signal Processing in Defence Conference*, Brighton, UK, May 2019.

[110] S. Weiss, S. Redif, T. Cooper, C. Liu, P. Baxter, and J. McWhirter.
Paraunitary oversampled filter bank design for channel coding.
*EURASIP Journal on Advances in Signal Processing*, 2006:1–10, 2006.

[111] S. Weiss, J. Selva, and M. Macleod.
Measuring smoothness of trigonometric interpolation through incomplete sample points.
In *EUSIPCO*, 2020.

[112] S. Weiss, C. H. Ta, and C. Liu.
A wiener filter approach to the design of filter bank based single-carrier precoding and equalisation.
In *IEEE International Symposium on Power Line Communications and Its Applications*, pages 493–498, Pisa, Italy, March 26-28 2007.

[113] S. Weiss, P. Yarr, W. Al-Hanafy, A. Millar, and C.-H. Ta.
An oversampled modulated filter bank transmultiplexer with precoding and equalisation.
In *Third Workshop on Power Line Communications*, Udine, Italy, October 2009.